（論文題目）

Iterative interaction between muscle and nerve cells after eccentric contraction-induced muscle damage

12N0001　　李　基赫

Kihyuk Lee

Iterative interaction between muscle and nerve cells after eccentric contraction-induced muscle damage

Kihyuk Lee

Graduate School of Health and Sport Science

Nippon Sport Science University

Contents

Chapter 1. Introduction

1-1. General introduction

Components of skeletal muscle

Skeletal muscle has the following functions such as movement, stability, and heat production. Skeletal muscle is composed by muscular tissues and fibrous connective tissues. Muscle tissue is made up with muscle fibers. Fibrous connective tissues include blood vessels and nerve fiber which are covered with the epimysium, perimysium, and endomysium (Figure 1-1). Muscle fibers are surrounded by the sarcolemma (Figure 1-2). The sarcolemma surrounds both sarcoplasm and muscle fibers. The sarcoplasm in the sarcolemma has the sarcoplasmic reticulum and T-tubule which are involved in the rise of action potential (Figure 1-3). Muscle fiber has multiple nuclei and is made up by nascent single nucleus muscle cell called myoblast. When myoblasts are fused, muscle fiber is formed. Satellite cells are muscle stem cells which is located between the muscle fiber and sarcolemma. If the muscle is damaged, they can supply new muscle fibers.

Each muscle fiber consists of myofibrils. The unit of myofibril is called sarcomere (Figure 1-4). There are thin filaments (actin) and thick filaments (myosin) in the sarcomere. The thin filament consists of actin, tropomyosin, and troponin. The thick

filament is made up of the myosin protein. Myosin has two heads which are twisted in the thick filament and located toward the thin filament. They can bind to actin in the thin filament. When myosin heads combine to actin, myofibril is contracted and force is generated.

Relationships of skeletal muscle and nerve

Skeletal muscle contracts when it is stimulated by somatic nervous system. If the somatic nervous systems cannot transmit signal to skeletal muscles, muscles are paralyzed. Therefore, in order to understand skeletal muscle contractions, the knowledge of relationship between muscle and nerve systems is needed. Skeletal muscles are regulated by motor neurons in the nervous system. Cell bodies of the motor neurons are located in the brain and spinal cord. They are called somatic motor nerve fibers and control the skeletal muscle. Somatic motor nerve fiber innervates more than two muscle fibers. The unit of nerve fiber and muscle fibers are called motor unit. It is important for controlling movement and strength exertion of the skeletal muscle. The spot where a nerve fiber connects to the muscle fiber is called the neuromuscular junction. When a signal of the nerve fiber reaches the neuromuscular junction, it stimulates the skeletal muscle fibers. As a result, skeletal muscles are contracted (Figure

1-5).

The stage of the muscle contraction can be explained by the following four major phases; 1) Excitation, 2) Excitation-contraction coupling, 3) Contraction, and 4) Relaxation. When action potential in the nerve fiber arrives to the end of motor neuron, acetylcholine is released. Released acetylcholine combines to the receptors on the motor end plates. As a result, action potentials in the nerve fiber elicit action potentials in the muscle fiber. This stage is called 1) Excitation (Figure 1-5, ①). Action potential in muscle fiber is transmitted to T-tubule. Sarcoplasmic reticulum releases calcium ions and then combines with the troponin of the thin filaments. This link is called 2) Excitation-contraction coupling (Figure 1-5, ②~③). 3) Contraction is a stage where muscle fiber creates tension and is shortened. This stage is where tropomyosin shifts and expose myosin binding site. As a result, thin filaments (myosin) pulls in thick filaments (actin). Sarcomere is shortened and muscle fiber is contracted (Figure 1-5, ④). When the signal of the nerve fiber cannot transmit to the neuromuscular junction, contraction is finished and muscle fiber returns to its original length. This stage is called 4) Relaxation (Figure 1-5, ⑤~⑦).

The nervous system and consisting cells

The nervous systems can be practically divided into central nervous system (CNS) and peripheral nervous system (PNS). CNS consists of the brain and the spinal cord. PNS includes the nerves and ganglia except CNS. PNS connect CNS to the target tissues/organs. PNS is divided into the somatic nervous system, the sensory nervous system, and the autonomic nervous system. From the three nervous systems mentioned above, the somatic nervous system is associated with the voluntary control of the body movements via skeletal muscles.

Nervous tissue is composed of nerve cells and glial cells. Nerve cell transmits information electrically and chemically. Nerve cell is frequently called neuron. Glial cell directly contacts with the nerve cells and often surround them. Neuron basically consists of cell body, axon, and many dendrites. Dendrites receive information from another cell and transmit the message to the cell body. The cell body contains the nucleus, mitochondria and other cell organelles. The signals from the cell body are transmitted by the axon. Nerve cells are divided into three types. First is the sensory neuron which has a long dendrite and short axon. It carries signals to the CNS. Second is the motor neuron which has a long axon and short dendrites and transmits signals to the muscles. Third is the interneuron which transmits neuron to neuron in the CNS.

On the other hand, glial cells serve as a supportive role in neural tissue. In PNS, most axons are surrounded by the myelin sheath. The specialized glial cell called the Schwann cell is supportive and nutritive to the neuron [1] (Figure 1-6).

Types of skeletal muscle injury

Skeletal muscle injuries are caused by physical exercise when skeletal muscle is overused and/or over stretched. Main muscle injuries caused by body movement are muscle soreness and muscle strain. Muscle soreness accompanies pain and is divided into acute muscle soreness and delayed onset muscle soreness. Acute muscle soreness is one form of exercise-induced muscle damage. Although acute muscle soreness occurs immediately after exercise and continues to pain for several minutes, pain of delayed onset muscle soreness appears between 24 hours and 72 hours after exercise. The causes are accumulation of chemicals, edema, and muscle fatigue.

Muscle strain is tears of muscle fibers and damages which occur in both muscle and tendon. Tendon is fibrous tissues and connects muscle and bone. Muscle strain is caused by overuse of muscle and tendon and also as a result of overstretching and/or excessive muscle contraction during exercise like eccentric contraction. The main part where the strain occurs is the hamstrings. Strain accompanies pain, swelling,

inflammation, and weakness. More severe strain experiences loss of muscle function. Strains are divided into three grades (Table 1-1). First grade is the mild strain. Some muscle fiber is damaged and can be recovered within two weeks. Second grade is also damaged muscle fibers. Recovery is accomplished by more than four weeks. Third grade is a severe injury with ruptured muscle fibers. About six month periods are required for recovery.

Types of peripheral nerve injury

As depicted above, nerve tissues consist of neural cells and glial cells. In PNS, Schwann cells make myelin sheath and surround nerve cell axon (Figure 6). When peripheral nerve injury occurs, axon and/or myelin sheath might be damaged. According to the Seddon's classifications [2] (Figure 1-7), peripheral nerve injury is divided into three types, such as neurapraxia, axonotmesis and neurotmesis. Neurapraxia is temporary damage to the myelin sheath but the nerve cell axon and Schwann cell remains intact. Since it is an impermanent injury, the myelin damage can be repaired. Axonotmesis is a damage of the nerve cell axon. Compared with neuropraxia, both myelin sheath and axon are damaged. Because the Schwann cell remains intact, damaged myelin sheath and axon can be regenerated. By a more severe crush or

contusion, the nerve tissue is damaged. Neurotmesis is an entire disruption or damage of the nerve fiber. It is the most critical nerve injury and means the severance of the nerve fiber. Unlike the CNS, regeneration is possible in the PNS, and, in that case, Schwann cell plays an important role in damaged peripheral nerve regeneration [3-5].

1-2. Mechanism of the skeletal muscle protein degradation after eccentric contractions

Eccentric contractions cause a skeletal muscle injury

Skeletal muscle contractions are divided into the following three types, isometric contraction, concentric contraction and eccentric contraction. Isometric contraction is a muscle contraction without change in the muscle length. Because isometric contraction is maintained in astatic position, a range of motion does not change. However, muscle length shortens when muscle is concentrically contracted. Eccentric contraction (EC) is the opposite of concentric.

Since exerting force of eccentric contraction is the largest among three types of muscle contractions, the diverse effects of eccentric contractions have been reported [6-8]. Because the contracting muscle is forcibly lengthened during ECs, more and more sarcomeres will become overstretched [9], beginning with the weakest and progressively including stronger sarcomeres. Moreover, when ECs are repeated, more and more sarcomeres become disrupted. Disrupted sarcomeres lead to structural distortions and membrane damage of sarcoplasmic reticulum, transverse tubules, or the sarcolemma [6]. This is accompanied by the uncontrolled release of Ca^{2+} and

dysfunction of the excitation-contraction (E-C) coupling system, triggering the damage process [10-12]. If the damage was extensive enough, muscle fibers would die and lead to local inflammatory response associated with tissue edema and soreness [13]. Generally, this muscle damage is characterized by sustained loss of muscle force and range of motion, histologic disturbance of muscle and connective tissue, large decreases of muscle proteins and oxidative stress in the blood, shift in optimum length, fall in active tension, rise in passive tension and development of delayed-onset muscle soreness (DOMS) and swelling [6, 11, 14-16].

Among the injuries by ECs, muscle strain injury is not the result of muscle contraction alone, rather, strains are the result of excessive stretch while the muscle is being activated [17]. ECs impose a greater amount of tension on the active muscle. In particular, high-speed ECs seem to exert an additional effect on muscle tension. Thus, ECs induces both muscle hypertrophy and muscle damages [8, 18-21]. Furthermore, severe ECs with larger range of motion and/or faster contraction velocity tend to induce severe muscle damage [7, 22, 23]. In fact, Song [24] and Ochi et al. [25] showed that ECs with a larger range of motion and/or faster angular velocity cause functional and histological damage to the rat gastrocnemius muscle. For this reasons, severe ECs have been considered to induce muscle strain injury.

The mechanism of the skeletal muscle degradation

In previous study, Ochi et al. [25] have reported that severe ECs induce skeletal-muscle protein degradation. Muscle atrophy occurs when there is an imbalance between protein degradation and synthesis. Skeletal muscle atrophy happens when muscle protein degradation exceeds synthesis [26]. It has been reported that there are four mechanisms in protein degradation [27] (Figure 1-8). The first mechanism is the ubiquitin-proteasome system. The second is the autophagy-lysosome system. The third is the calpain system. The fourth is the caspase system. It has been reported that the ubiquitin-proteasome system is the major cause to skeletal muscle atrophy [28]. The ubiquitin-proteasome system induces protein degradation by up-regulation of two ubiquitin-protein ligase, muscle-specific ubiquitin ligases muscle atrophy F-box (MAFbx, another name is an atrogin-1) and muscle RING finger 1 (MuRF1) [29, 30]. Furthermore, the expression of MAFbx is regulated by forkhead box O (FoxO) of transcription factor [31].

When the inactivated FoxOs located in the cytoplasm becomes dephosphorylated, it moves to the nucleus for transcription of MAFbx and MuRF1. (Figure 1-9). Moreover, the expression of FoxOs results from decreased activation of Akt/mammalian target of rapamycin (mTOR)/p70s6k signaling pathway which activates protein synthesis making

it to an anabolic states [32, 33]. The Akt signaling pathway is a positive regulator of muscle protein synthesis and muscle hypertrophy [34, 35]. As a result, phosphorylated FoxOs suppress protein degradation and promote protein synthesis [32]. On the contrary, the expression of FoxOs in the nucleus stimulates protein degradations.

Another regulator of MAFbx and MuRF1 is the myostatin [36, 37]. Myostatin belongs to the member of transforming growth factor (TGF)-beta superfamily [38] and is a negative regulator of muscle hypertrophy [39]. Mutation of myostatin has been reported to result in growth of muscle mass [40]. In addition, myostatin has been reported to inhibit myoblast differentiation and myotube growth [41] and regulates FoxO1- dependent mechanism [36] (Figure 1-9). Moreover, the expression of myostatin stimulates protein degradation and suppresses protein synthesis [41, 42]. In previous study, Ochi et al. have reported that ECs with 180°/s angular velocities induce higher expression levels of FoxO1, FoxO3a and myostatin [25]. Furthermore, they observed that ECs with slower angular velocity (30°/s) did not induce the expression of FoxO proteins. Because these proteins lead to degradation of muscle proteins, 180°/s ECs might induce muscle atrophy. However, the mechanism of inducing muscle protein degradation by ECs has not been elucidated.

The possibility of skeletal muscle degradation following AMPK activation after eccentric contractions

5′-AMP-activated protein kinase (AMPK), a well-characterized sensor of cellular energy state [43-45], consists of three subunits, namely, a single catalytic domain (α) and two regulatory domains (β and γ). Phosphorylation of the α-subunit is required for AMPK activation, which initiates transcriptional and metabolic events that generate AMP and inhibit ATP-consuming processes. In skeletal muscle, AMPK is activated by a variety of ATP-consuming stimuli, such as exercise [46], electrical stimulation [47] and glucose deprivation [48].

Recent reports have suggested that AMPK activation inhibits myoblast differentiation, protein synthesis, and hypertrophy in skeletal muscle [49-54]. Treatment with the AMPK activator, 5-Aminoimidazole-4-carboxamide ribonucleotide (AICAR), has been shown to stimulate expression of the MAFbx and MuRF1 [51]. Moreover, AMPK activation by AICAR treatment is known to inhibit contraction-induced activation of mTOR [52] and hypertrophy [49] in rat skeletal muscles. Furthermore, the activation of AMPK in C2C12 cells has been shown to reduce myotube formation [50], induce degradation of myofibrillar protein, and stimulate expression of the transcription factors MAFbx and FoxO [54]. In addition, skeletal muscle hypertrophy in AMPKα1

knockout mice suggests that AMPK plays an important role in limiting muscle growth [53].

Ochi et al. have recently shown that eccentric contractions (ECs) induce expression of the atrophy-related factors FoxO1, FoxO3a, and myostatin in rat's gastrocnemius muscle [25]. Although the molecular mechanisms underlying these events are uncertain, as described above, FoxO transcriptional factors and other atrophy-related factors have been shown to be induced by activation of AMPK. Furthermore, binding assays have demonstrated the presence of functional binding sites for FoxO1 and SMADs in the myostatin promoter [55]. These lines of evidence suggest that induction of the expression and activity of FoxO transcriptional factors in response to AMPK activation stimulates myostatin levels, resulting in muscle atrophy.

Therefore, in chapter 2, I hypothesized that AMPK plays a key role in regulating the expression of atrophy-related factors in rat gastrocnemius in response to ECs with severe ankle joint torque deficit.

1-3 Skeletal muscle and peripheral nerve damages following eccentric contractions

Relationships between eccentric contractions and a peripheral nerve injury

Although muscles are composed of various tissues, including muscle fibers, blood vessels, and nerves, research on muscle injury has generally focused on damage only to muscle tissues. However, muscle damage induced by ECs has reportedly produced alterations in peripheral nerve function such as changes in excitation-contraction (E-C) coupling and in motor unit recruitment [12, 56-58]. With regard to muscle injury, Kami et al. [59] showed that muscle contusion injuries cause not only muscle damage but also injury to nerve cells. They found up-regulation of neurotrophic factors and their receptors in motor neurons and Schwann-like cells in damaged muscle, similar to those found after nerve transection. This suggested that inflammatory reactions in damaged non-neuronal tissues might facilitate nerve damage. Similarly, overstretching, disruption, and inflammation of muscle fibers by ECs may damage nerve cells. This phenomenon has not been examined previously. Furthermore, since nerve damage leads to the reduction of muscle strength and muscle atrophy, there is a possibility that nerve damages occur especially in severe muscle damages.

Roles of schwann cell, macrophages and neurotrophins under nerve injury and repair

Nerve tissues consist of neural cells and glial cells. In the PNS, Schwann cell is one of the glia cells. They make myelin sheath and surround nerve cell axon. Unlike in the CNS, regeneration in the PNS is possible. When peripheral nerve injury occurs, axons and/or myelin sheaths are damaged [1, 60]. Schwann cells play an important role in regeneration of damaged peripheral nerves [3-5]. During PNS development and regeneration, Schwann cells ensheath individual axons and eventually form the myelin sheath [1]. Schwann cell migration is essential for responses to tissue damage after injury [61]. At the same time, macrophages infiltrate in order to remove debris, specifically myelin and damaged axons, from the injury site [5, 62, 63]. Macrophages do not phagocytose all cellular debris at the nerve injury site [64] but rather select and salvage damaged myelin and axons [60, 65, 66]. In addition to Schwann cells, neurotrophins play multiple roles in the development of the peripheral nervous system, and they contribute to Schwann cell survival, growth, and differentiation [3, 61, 67, 68]. Neurotrophins include nerve growth factor (NGF), brain-derived neurotrophic factor (BDNF), neurotrophin 3 (NT-3), and neurotrophin 4/5 (NT-4/5). They are activated by the tropomyosin-receptor-kinases (Trks). NT-3 activation of TrkC induces Schwann cell

migration through the c-jun N-terminal kinase pathway [61]. After peripheral nerve injury, neurotrophic factors are upregulated and contribute to successful regeneration [69, 70].

Measure of nerve conduction velocity

Nerve conduction velocity (NCV) is one of the measurement methods that is used to diagnose neuromuscular diseases and damage [71, 72]. As mentioned above, muscle damage that is induced by ECs has reportedly produced functional alterations in muscle spindle and motor units [12, 56-58]. The overstretching, disruption, and inflammation of muscle fibers by ECs may possibly damage nerve tissue. The measurement of NCV is an available method for determining functional nerve damage following ECs. Therefore, in order to confirm nerve damage, it is important to examine whether NCV is changed after ECs. As with NCV, assessments of these various factors and pathways can be used to measure peripheral nerve damage. Although it has been reported that exercise training improves NCV after sciatic nerve crush [73, 74], no studies have examined whether ECs affect NCV. The hypothesis of chapter3 is that excessive ECs causing muscle protein degradation induces structural damage and functional deficits of the sciatic nerve and its branches.

1-4 Causes of the skeletal muscle atrophy by nerve damage

Skeletal muscle atrophy is dependent on muscle fiber type in nerve damage

Skeletal muscle atrophy is a result of disuse, aging, and diseases. Many researchers have reported about the mechanism of skeletal muscle atrophy. In general, experiments about the mechanism of skeletal muscle atrophy have been conducted using an immobilization and denervation model. In addition, the fashion of skeletal muscle atrophy seems to be dependent on muscle fiber type. Muscle fiber types are categorized into two main types due to metabolic activity. The first type is slow-twitch fibers (type1) and the other type is fast twitch fibers (type2). Slow-twitch fibers and fast twitch fibers are called oxidative muscle fibers and glycolytic muscle fibers, respectively. Moreover, fast twitch fibers can be divided into two types: type2A and type2B. Although the mechanism of fiber-specific muscle atrophy is unclear, it has been reported that immobilization induces skeletal muscle atrophy due to disuse and mainly decreasing muscle fibers which are slow-twitch fibers. On the other hand, the atrophy of fast-twitch fibers is attributed to denervation which in result causes loss of motor neuron. The molecular mechanism and phenomenon about muscle atrophy using inactivity and denervation model have been reported. However, the mechanism of muscle atrophy

following nerve damage remains poorly understood.

Relationship between nerve crush injury and muscle damage

Nerve injury has been reported to be the cause of skeletal muscle atrophy [75]. Especially, the denervation of skeletal muscle has been researched to investigate the mechanism of muscle atrophy. Although many studies observed that the denervation triggers expression of atrophy-related factors (MAFbx, MuRF1, FoxO1, FoxO3a, and myostatin), molecular mechanisms of denervation have not been well understood. Moreover, Nerve crush injury (NCI) is one type of the nerve damage and NCI is similar to neuropraxia or axonotmesis according to the Seddon's classifications (Figure 1-7). However, the molecular mechanism of the NCI has not been sufficiently elucidated. Although one group reported that NCI induces the expression of myostatin, why myostatin increases is not yet known. In chapter 2 and 3, I observed that AMPK activated by ECs stimulate the expression of FoxO1, FoxO3a, and myostatin which causes muscle protein degradation. Thus, ECs might induce nerve damage as well as muscle damage. Since nerve damages including denervation trigger the muscle atrophy by protein degradation, if AMPK activation is result of nerve damage, it can be evidence that ECs induce nerve damage. Since model of denervation for nerve damage might be similar to a type of neurotmesis according to the Seddon's classifications (Figure 1-7), it

does not coincide with induced nerve damage by ECs. However, model of NCI might be similar to nerve damage induced by ECs. Therefore, I hypothesized that NCI activates AMPK and regulates the expression of FoxO1, FoxO3a, and myostatin as denoted in chapter 2.

1-5 Table and Figures

	Grade1	Grade2	Grade3
Pain	*	**	***
Weakness	X	O	O
Loss of function	X	X	O
Symptom		Swelling Tenderness	Swelling Tenderness Dislocation
Recovery period	Within two weeks	About four weeks	About six month

Table 1-1. Grades of muscle strain

Strains are divided into three grades. First grade is a mild strain. Some muscle fiber is damaged and can recover within two weeks. Second grade is also damaged muscle fibers. Recovery is accomplished by more than four weeks. Third grade is a severe injury with ruptured muscle fibers. About six months of periods is required for recovery.

http://www.radiologyassistant.nl/en/p4a47de30059ba/muscle-mr-traumatic-changes.html

http://www.humankinetics.com/excerpts/excerpts/understanding-muscle-strains

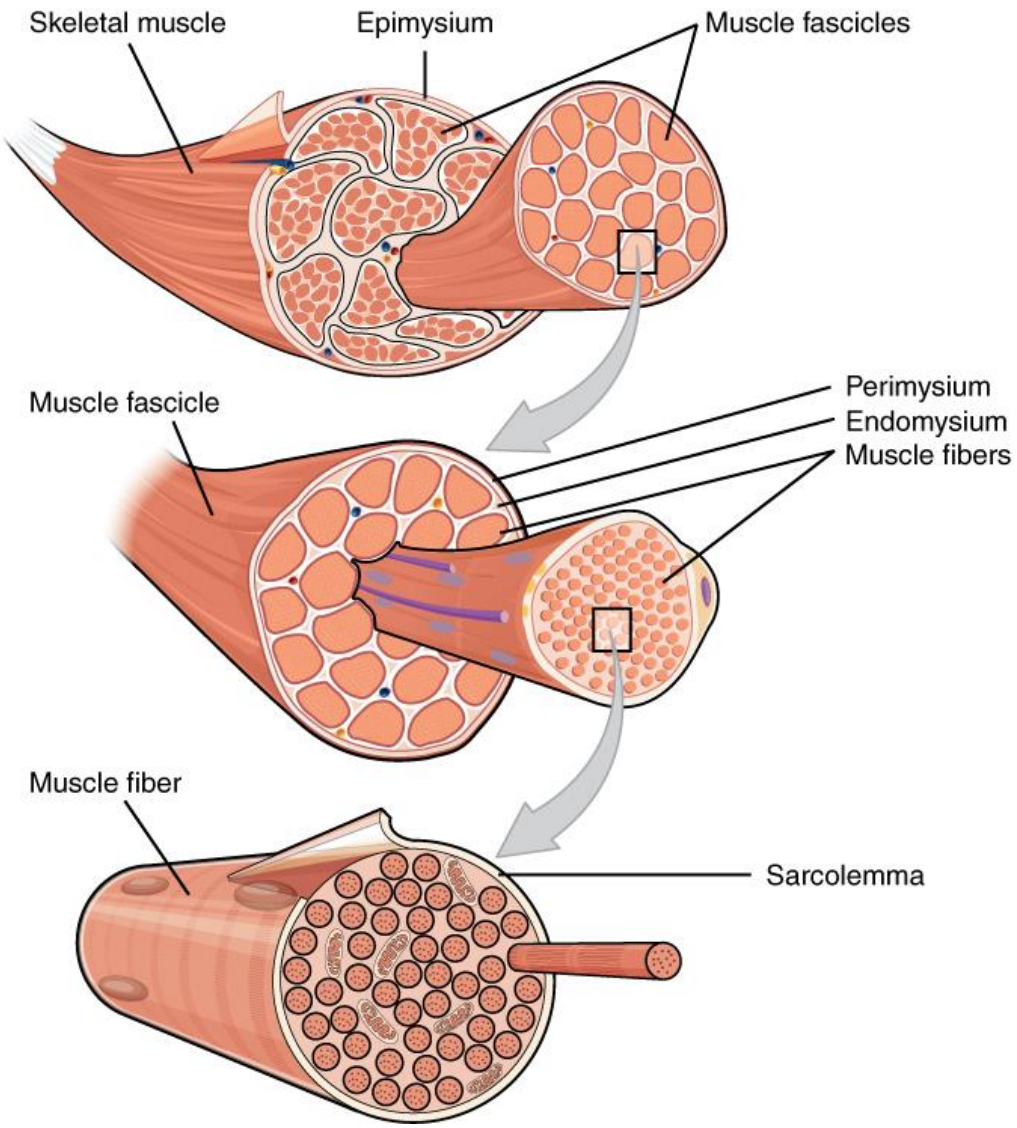

Figure 1-1. The division of tissue layers of skeletal muscle

Skeletal muscle is made up with muscular tissues (muscle fibers) fibrous connective tissues and muscle fibers which are covered with sarcolemma.

http://cnx.org/contents/14fb4ad7-39a1-4eee-ab6e-3ef2482e3e22@7.1:65/Anatomy_&_Physiology

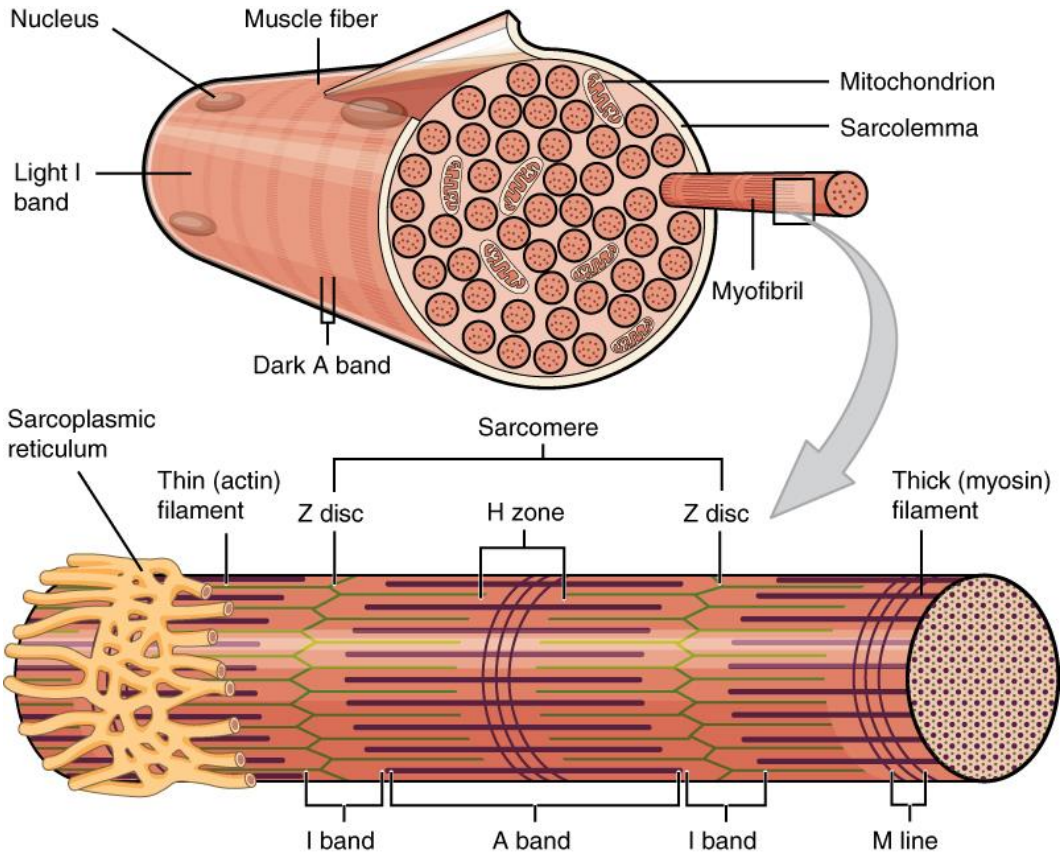

Figure 1-2. The components of muscle fiber

Muscle fiber is filled by myofibril and sarcoplasm. The sarcoplasmic reticulum and T-tubule are located in sarcoplasm

http://cnx.org/contents/14fb4ad7-39a1-4eee-ab6e-3ef2482e3e22@7.1:65/Anatomy_&_Physiology

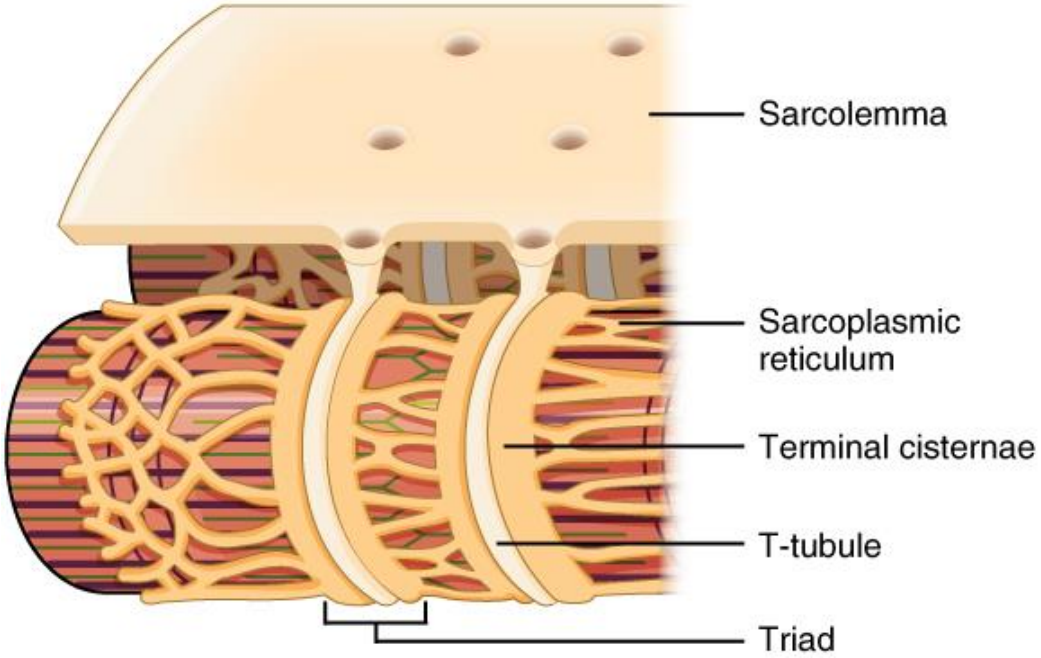

Figure 1-3. The structure of sarcolemma and role of T-tubule and Sarcoplasmic reticulum

The action potential in muscle fiber is transmitted to T-tubule and then Sarcoplasmic reticulum releases calcium ions for muscle contraction.

http://cnx.org/contents/14fb4ad7-39a1-4eee-ab6e-3ef2482e3e22@7.1:65/Anatomy_&_Physiology

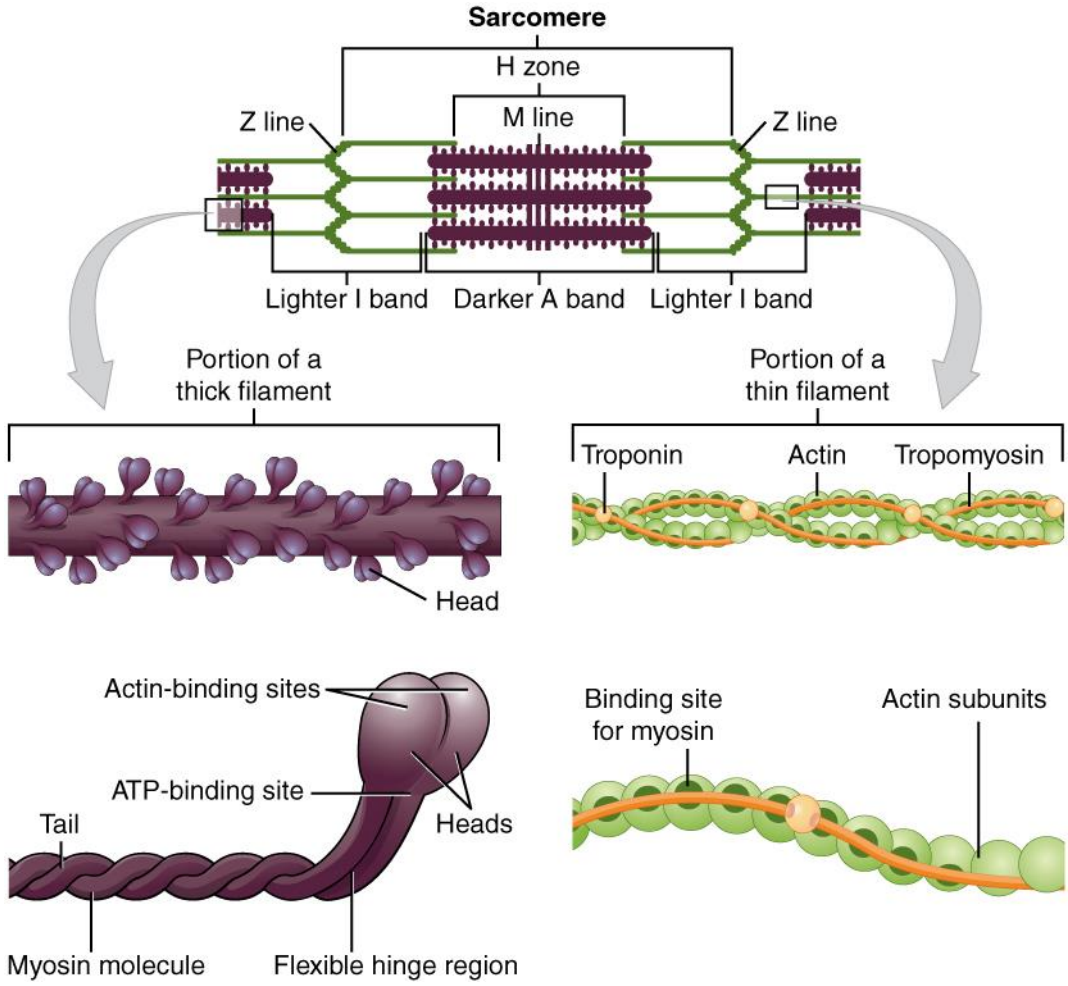

Figure 1-4. The structure of sarcomere and myofibril (thick and thin filament)

The thin filament consists of actin, tropomyosin, and troponin and the thick filament is made up of the myosin protein. When myosin heads combine to actin, myofibril is contracted and force is generated.

http://cnx.org/contents/14fb4ad7-39a1-4eee-ab6e-3ef2482e3e22@7.1:65/Anatomy_&_Physiology

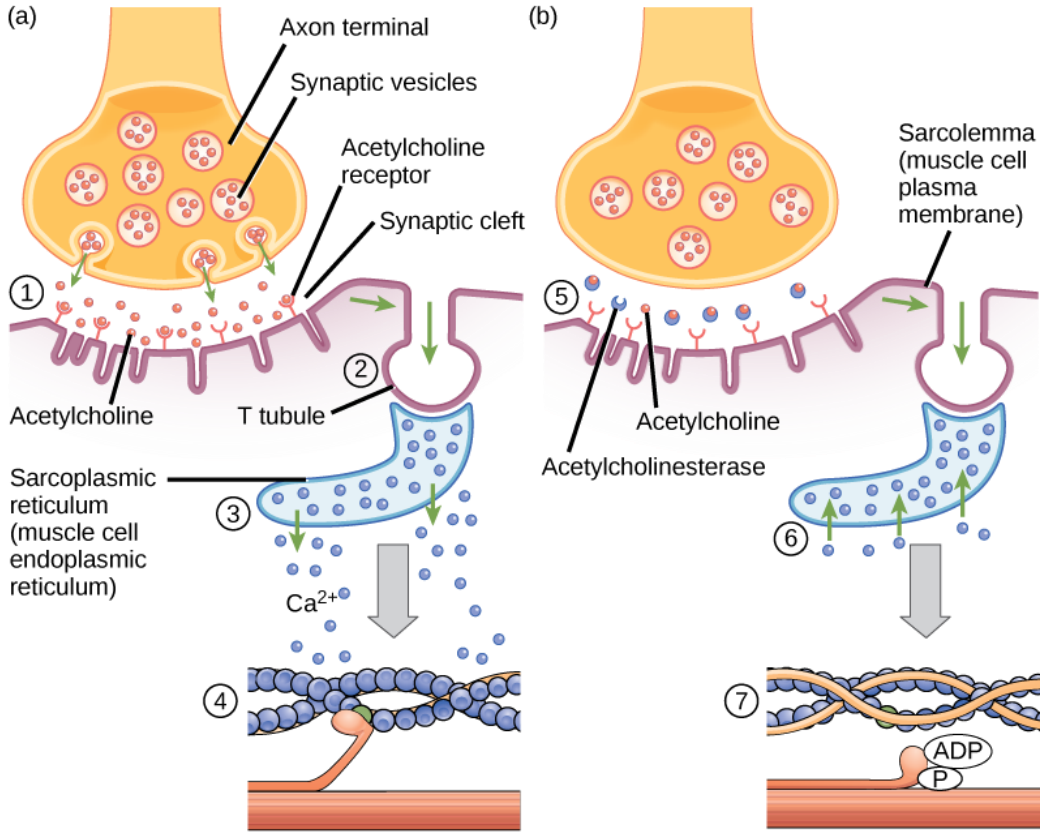

1. Acetylcholine released from the axon terminal binds to receptors on the sarcolemma.
2. An action potential is generated and travels down the T tubule.
3. Ca^{2+} is released from the sarcoplasmic reticulum in response to the change in voltage.
4. Ca^{2+} binds troponin; Cross-bridges form between actin and myosin.
5. Acetylcholinesterase removes acetylcholine from the synaptic cleft.
6. Ca^{2+} is transported back into the sarcoplasmic reticulum.
7. Tropomyosin binds active sites on actin causing the cross-bridge to detach.

Figure 1-5. The stage of muscle contraction through nerve impulse transmission

The stage of muscle contraction can be explained by the following four major phases; 1) Excitation (①), 2) Excitation-contraction coupling (②~③), 3) Contraction (④), and 4) Relaxation (⑤~⑦).

https://www.boundless.com/biology/textbooks/boundless-biology-textbook/the-musculoskeletal-system-38/muscle-contraction-and-locomotion-218/excitation-contraction-coupling-828-12071/images/fig-ch38_04_06/

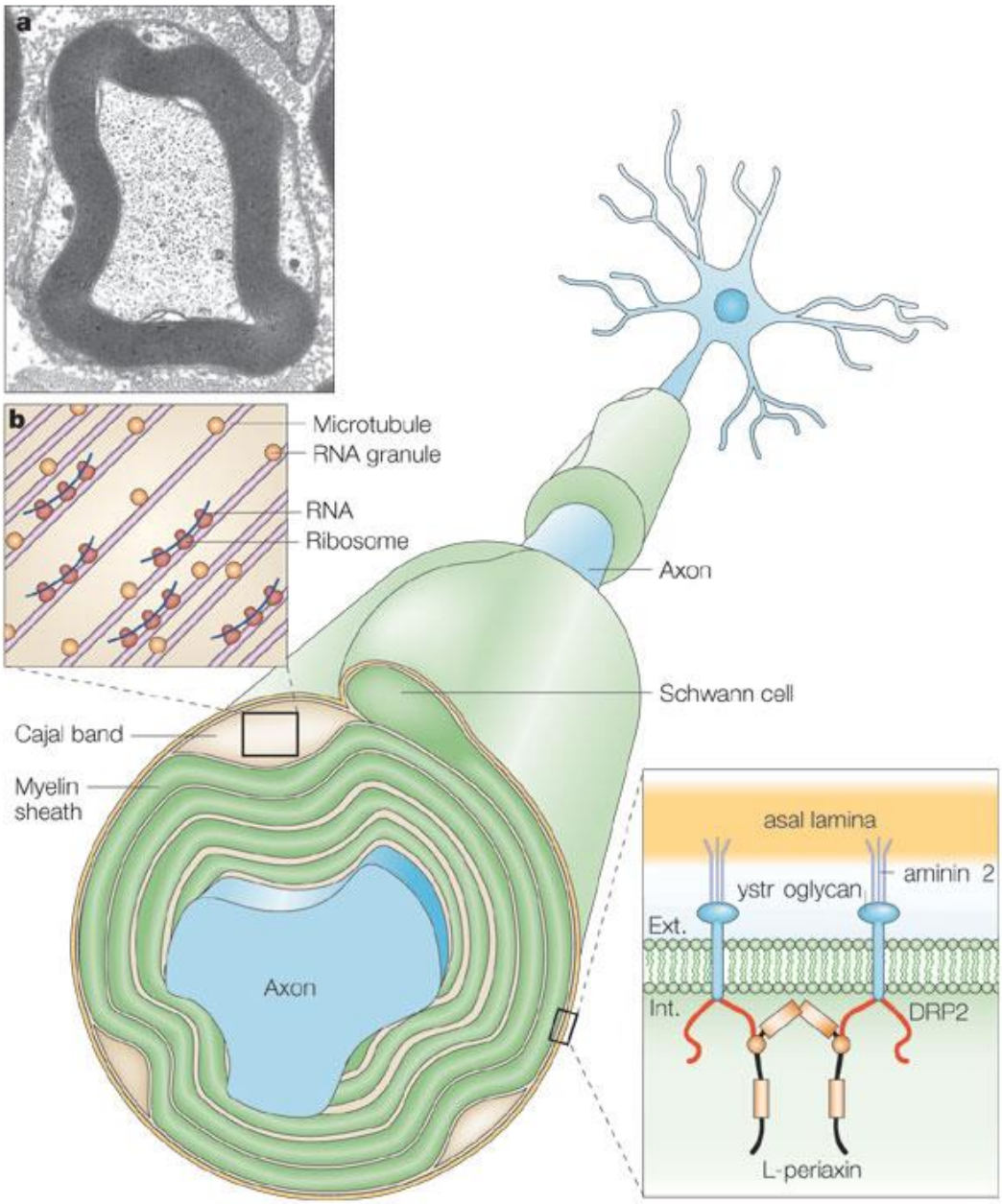

Figure 1-6. The cross section of myelin sheath and axon

In PNS, axons are wrapped in a myelin sheath formed from the plasma membrane of Schwann cell [1].

http://www.nature.com/nrn/journal/v6/n9/full/nrn1743.html

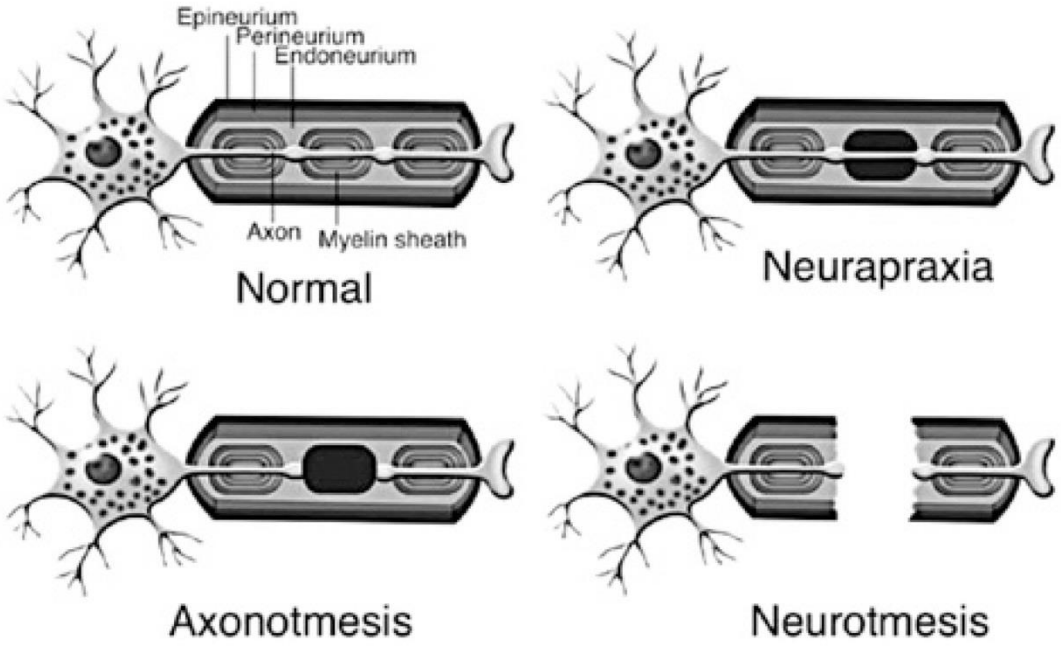

Figure 1-7. Seddon's classification about nerve injury

According to Seddon's classification [2], grades of nerve injury are divided into three grades [76].

http://www.scielo.br/img/revistas/anp/v71n10/0004-282X-anp-71-10-0811-gf01.jpg

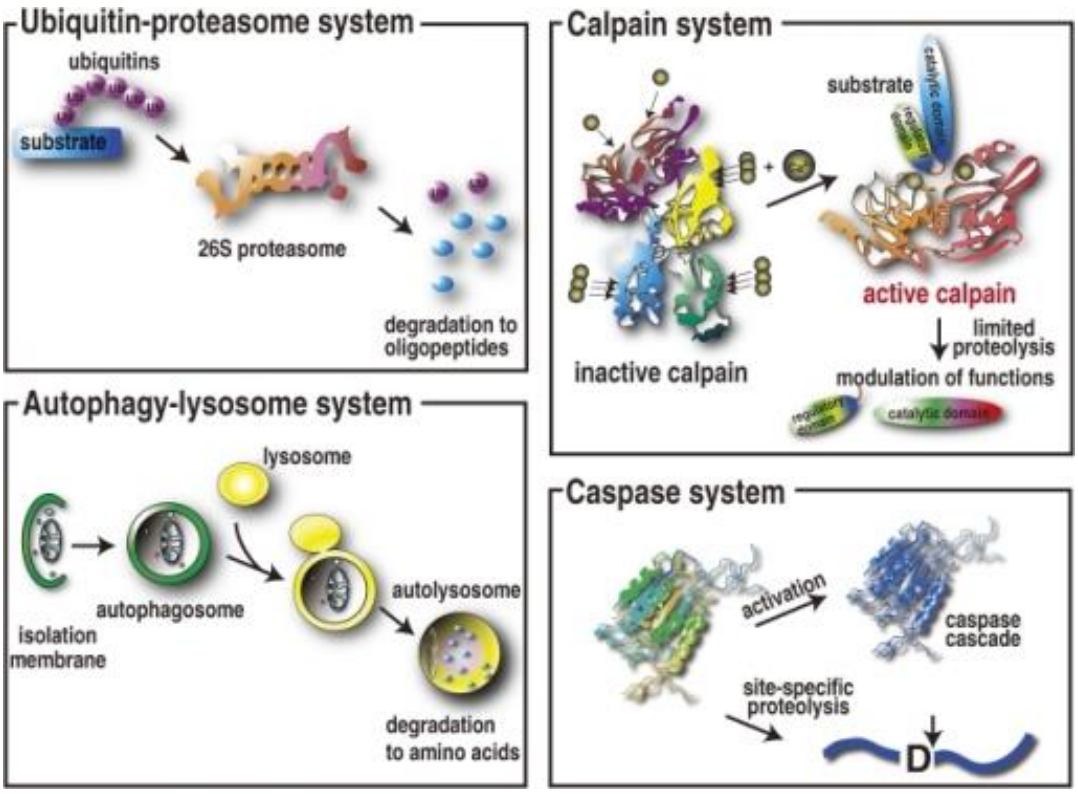

Figure 1-8. **Major protein degradation systems**

It has been reported that there are four mechanisms in protein degradation [27].

http://openi.nlm.nih.gov/detailedresult.php?img=3153876_pjab-87-287-g002&req=4

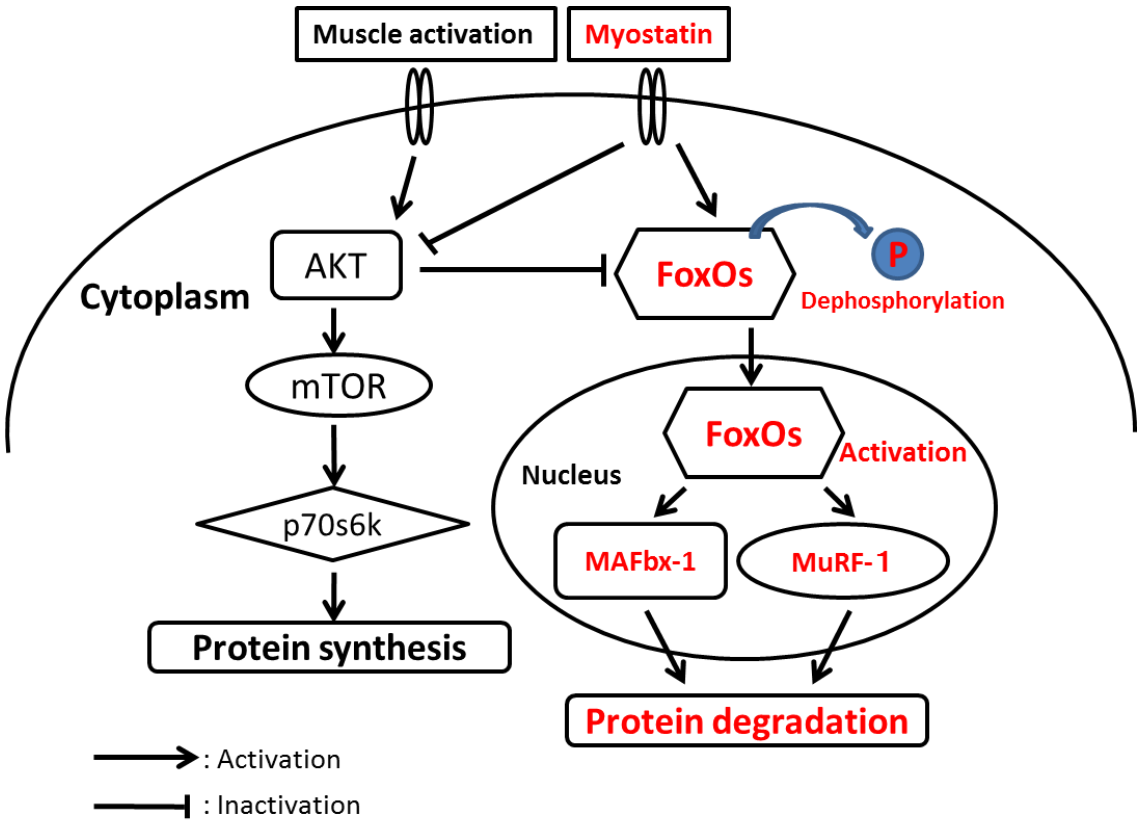

Figure 1-9. Molecular mechanisms of protein synthesis and degradation in skeletal muscle

Muscle activation induces protein synthesis and suppresses protein degradation. On the contrary, myostatin stimulates protein degradation and inhibits protein synthesis.

Chapter 2.

The possible role of AMP−activated protein kinase (AMPK) in skeletal muscle degradation after eccentric contractions

2-1 Purpose

The purpose of this study was to investigate what the cause was for inducing muscle protein degradation by ECs. In this study, I hypothesized that AMPK plays a key role in regulating the expression of atrophy-related factors in rat gastrocnemius in response to ECs with severe ankle joint torque deficit. To evaluated the effect of ECs, the expression levels of phosphorylated AMPK and phosphorylated Acetyl CoA carboxylase (ACC), which are well-known markers for AMPK activation [52], and expression levels of FoxO1, FoxO3a, and myostatin were measured. Also,, changes in the levels of phosphorylated FoxO1, FoxO3a, and myostatin in L6 myotube cells in response to treatment with AICAR was measured.

2-2 Materials and Methods

Animal Care

Male Wistar rats (age, 11 weeks; body mass, 344–398 g; n = 18) were randomly assigned to the following three groups: a 180EC group (180EC; eccentric contractions with 180°/s angular velocity; n = 6), a 30EC group (30EC; eccentric contractions with 30°/s angular velocity; n = 6), and a control group (CON; n = 6). The angular velocities in the 180EC and 30EC groups were chosen in accordance with conditions set in previous study [25]. The rats were individually housed in ventilated cage (IVC) systems (Tecniplast, Milan, Italy) maintained at 22–24°C with a 12-h light/dark cycle. Rats were provided water and food ad libitum. No significant differences were found in weight between the groups (Data not shown). At 7 days after ECs, 6 rats in each group were dissected and weighed. This study was approved by the Ethical Committee for Animal Experiments at the Nippon Sport Science University.

Measurement of ankle joint torque

Ankle joint torque was measured as previously reported [77]. In brief, the right hind limbs of all the animals were shaved, and each rat was then anesthetized with

isoflurane. (aspiration rate, 450 mL/min; concentration, 2.0%). The anesthetized animals were used for isometric tetanic torque. Measurements were made before ECs and on days 1, 2, 3, 5, and 7 after ECs. For the control rats, only ankle joint torque was measured.

ECs of the medial gastrocnemius muscle

The EC system of the medial gastrocnemius muscle was similar to that observed in previous study [25, 77, 78]. After measurement of the ankle joint torque, the 180EC and 30EC groups were anesthetized and placed prostrate on the isokinetic dynamometer. The triceps surae muscle of the right hind limb was then electrically stimulated. ECs were induced at 180°/s (180EC) or 30°/s (30EC). The range of forced lengthening contraction was from 0° to 45°. The ECs comprised 4 sets of 5 contractions, and the interval between each set was 5 min. The control group was only anesthetized and no other treatment was received. After the last measurement of ankle joint torque, the muscle specimens were dissected, weighed, immediately frozen in liquid N_2, and stored at –80°C until analysis.

Cell culture

L6 rat myoblasts obtained from the Japanese Collection of Research Bioresources were grown in Dulbecco's modified Eagle's medium (DMEM) + 10% fetal bovine serum. Fusion of subconfluent myoblasts was induced by changing the medium to DMEM + 3% horse serum for seven days. Prior to initiation of the experiments, L6 myotubes were incubated in serum-free DMEM for 24 h. AICAR was added to the medium at a final concentration of 0, 0.1, 0.5, 1, 1.5, and 2 mM, and cells were maintained for 24 h. For western blot analysis, cells were harvested by scraping in RIPA buffer (#9808; Cell Signaling Technology, Danvers, MA, USA) and homogenized with a protease and phosphatase inhibitor cocktail (#78441; Thermo Scientific, Rockford, USA).

Western blotting analysis

The medial gastrocnemius muscle was macerated in liquid N_2 and homogenized in a buffer containing 50 mM Tris-Cl (pH 7.4), 150 mM NaCl, 5 mM ethylenediaminetetraacetic acid (EDTA), 0.5% sodium dodecyl sulfate (SDS), 1% deoxycholate, 0.1% Triton X-100, 1% Nonidet P-40 (NP-40), 0.05% mercaptoethanol, 10 mg/mL phenylmethylsulfonyl fluoride (PMSF), 0.5 mg/mL leupeptin, 0.2 mg/mL

aprotinin, and 1 mM Na3VO4. The homogenate was centrifuged at 16,000 ×g for 15 min at 4°C. Protein concentrations were determined using a protein concentration determination kit (Protein Assay II; Bio-Rad, Richmond, VA). A 30-μg (rat samples) or 20-μg (cell samples) total protein extracts from each sample were mixed with sample buffer, boiled, loaded on the same SDS-polyacrylamide gel (5 or 10%), and electrophoresed at 20 mA. The samples were electrophoretically separated at 180 mA for 90 min and separated proteins were then transferred onto polyvinylidene difluoride (PVDF) membranes (ATTO, Tokyo, Japan) or nitrocellulose membranes (GE healthcare, Whatman, Germany). The membranes were blocked for 1 h with phosphate-buffered saline (PBS) containing 5% skimmed milk and then incubated overnight at 4°C with the following primary antibodies (dilution, 1:1000): anti-AMPK alpha (#2532; Cell Signaling Technology), anti-p-AMPK alpha (Thr172) (#2535S; Cell Signaling Technology), anti-p-Acetyl-CoA Carboxylase (Ser79) (#3661S, Cell Signaling Technology), anti-FoxO1 (#9454S; Cell Signaling Technology), anti-p-FoxO1 (Ser256) (#9461S; Cell Signaling Technology), anti-FoxO3 (#2497S; Cell Signaling Technology), anti-p-FoxO3(Ser253) (#9466S; Cell Signaling Technology), anti-α-Tubulin (#2125; Cell Signaling Technology), and anti-myostatin (AB3239; Millipore, Billerica, MA). The membranes were then washed three times and incubated with the secondary

antibody at room temperature. Horseradish peroxidase (HRP)-conjugated goat anti-rat immunoglobulin G (IgG) or anti-rabbit IgG (dilution, 1:10,000) was used as the secondary antibody. Chemiluminescent reagents were used for detecting the secondary antibody (SuperSignal West Dura; Pierce Protein Research Products, Rockford, IL). Chemiluminescent signals were detected using a chemiluminescence detector (AE6961; ATTO) and quantified using a personal computer with image analysis software (CS Analyzer; ATTO). The band densities were expressed relative to those obtained for the control.

Statistical analysis

All values are expressed as mean ± standard deviations. One-way analysis of variance (ANOVA) followed by the Bonferroni test was used to compare the body mass, muscle wet weight, protein levels, and mechanical parameters with the exception of time course data. Two-way ANOVA followed by the Bonferroni test was used to test time course changes in ankle joint torque (time × groups). The significance level was set at $P < 0.05$.

2-3 Results

Body mass and muscle wet weights

No significant changes were observed between the groups with respect to either body mass or the wet weights of the medial gastrocnemius, lateral gastrocnemius, plantaris, and soleus muscles (Data not shown).

Effect of ECs on ankle joint torque

Figure 1 shows the isometric ankle joint torque deficit before and after ECs. Ankle joint torque was significantly lower in the 180EC group compared with the 30EC group at all times points (days 1, 3, and 5 post ECs, $P < 0.05$; day 2 post ECs, $P < 0.01$; Figure 2-1). In addition, compared with pretreatment values, significant torque deficit was observed in the 180EC group at all times points (day 1, 5, and 7 post ECs, $P < 0.05$; days 2 and 3 post-ECs, $P < 0.01$; Figure 2-1), whereas no such deficit was observed in the 30EC group.

Effect of ECs on AMPK levels and activity in medial gastrocnemius muscle

On day 7 post-ECs, the medial gastrocnemius muscle was removed for western

blot analysis. On day 7 post-180EC, levels of phosphorylated AMPKα in the 180EC group were significantly higher than those in the CON ($P < 0.05$) and 30EC ($P < 0.01$) groups (Figure 2-2A), while no significant differences were observed between CON and 30EC (Figure 2-2A).

Given that acetyl-CoA carboxylase (ACC) is a substrate for AMPK, levels of phosphorylated ACC are taken to reflect AMPK activity [52]. Compared with the CON group, levels of phosphorylated ACC at day 7 post-ECs were significantly higher in the 180EC ($P < 0.01$) and 30EC ($P < 0.05$) groups (Figure 2-2B).

Effect of ECs on FoxO1, FoxO3a, and myostatin levels in medial gastrocnemius muscle

Day 7 post-ECs levels of FoxO1 and FoxO3 were significantly higher in the 180EC group compared to the CON ($P < 0.001$, $P < 0.05$) and 30EC ($P < 0.01$, $P < 0.01$) groups (Figure 2-3A and 2-3C), whereas no significant difference was observed in the levels of phosphorylated FoxO1 and FoxO3a among all the groups (Figure. 2-3B and 2-3D).

Myostatin levels on day 7 post-ECs were significantly higher in the 180EC group compared with the 30EC ($P < 0.001$) and CON ($P < 0.01$) groups (Figure 2-4).

Effect of AICAR on levels of FoxO1, FoxO3a, and myostatin in L6 myotubes

Levels of the phosphorylated AMPK α subunit and phosphorylated ACC in L6 myotubes increased in an AICAR concentration-dependent manner (Figure 2-5A and 2-5B). Furthermore, relative contents of phosphorylated FoxO1 and FoxO3a to the total became lower in AICAR concentration-dependent manner (Figure 2-6A and 2-6B). Finally, levels of myostatin in L6 myotubes increased in an AICAR concentration-dependent manner (Figure 2-7).

2-4 Discussion

In previous study [25], although Ochi et al. found that FoxO1, FoxO3a, and myostatin were induced in response to severe (180°/s angular velocity) eccentric contractions with ankle joint torque deficit, the molecular mechanisms of this phenomenon were unclear. In this study, severe eccentric contractions were able to stimulate both overall phosphorylated levels and activity of AMPK up to day 7 post-180EC. I confirmed that the 180EC effect increases in day 7 post-ECs levels of FoxO1, FoxO3a, myostatin, as well as in phosphorylated AMPK-alpha and ACC. Indeed, even ECs without significant torque deficits (30EC group) induced ACC phosphorylation. Moreover, I have demonstrated that AMPK activation with AICAR in L6 myotubes reduces levels of phosphorylated FoxO3a and FoxO1 and increases myostatin levels, both in a concentration-dependent manner.

Since ACC is a substrate for AMPK, phosphorylated ACC content is associated with AMPK activity [52], and I hypothesized that ECs would elevate AMPK activity. AMPK is known to be activated by exercise, and the activation of AMPK is regulated by intensity of exercise [79-82]. Furthermore, a number of studies have suggested that regulation of skeletal muscle AMPKα1 and α2 differs depending on exercise intensity. AMPKα2 is activated during exercise at or above 60% VO2 peak [80, 82, 83], whereas

AMPKα1 is activated only during intense sprint-type exercise in humans [80-83]. Since Thomson et al. [52] and Atherton et al. [84] showed that muscle contraction with high electrical stimulation did not elicit total AMPKα phosphorylation and activation using rats, it is not determined if AMPKα phosphorylation and activation is dependent to intensity.

In this study of chapter 2, I confirmed that, as reported previously [25], FoxO protein levels are elevated on day 7 post-180EC. Since it has been reported that AMPK induces levels of FoxO proteins, muscle RING finger 1, and atrogin-1 *in vivo* and *in vitro* [51, 54, 85], I conclude that hyper activation of AMPK in the 180EC group supports elevated levels of FoxOs *in vivo*. Furthermore, I confirmed that myostatin levels on days 7 post-180EC were significantly higher compared to the CON and 30EC groups. Given that FoxO1 and SMADs bind to the myostatin promoter [55], I speculate that elevated levels of FoxO1 contribute to higher expression of myostatin in response to 180EC. With regard to the relationship between AMPK and myostatin, Chen et al. reported that AMPK is activated by myostatin, leading to the promotion of glycolysis [86]. Also, both expression and activity of AMPK in myostatin-null mutant mice was found to be higher than in wild-type mice [87]. However, from the previous study that reports AMPK regulate myostatin [88], I speculate that expression of myostatin is

induced by AMPK activation on day 7 post-180EC.

I used an *in vitro* cell culture system to examine the effects of the AMPK activator, AICAR, on levels of FoxO proteins and myostatin. Previous studies have shown that AICAR stimulates FoxO mRNA and protein expressions in C2C12 myotubes [54]. In contrast, another study showed that AICAR and another AMPK agonist, metformin, decreased FoxO mRNA levels in C2C12 myotubes [85]. Neither of these studies, however, analyzed the effect of AMPK agonists on levels of phosphorylated FoxO proteins. It has been shown that AICAR decreases levels of phospho-FoxO3a in the cytoplasm of C2C12 cells, suggesting that FoxO3a may relocate to the nucleus in these cells [89]. Moreover, AICAR treatment has been demonstrated to attenuate rat cardiomyocyte hypertrophy and to effect a decrease in the ratio of the phosphorylated: unphosphorylated forms of FoxO1 [90].

In this study, I found that levels of phospho-FoxO1 and phospho-FoxO3a were down-regulated in an AICAR concentration-dependent manner, suggesting that activated AMPKs regulate the relative phosphorylated states of FoxO1 and FoxO3a in rat L6 myotubes. This result is in agreement with a previous study [89] showing that AICAR treatment of C2C12 myotubes activated AMPK and decreased FoxO3a phosphorylation, although this study did not examine overall FoxO1 levels or levels of

phospho-FoxO1. Using an *in vitro* kinase assay, Greer et al. showed that activated AMPK resulted in specific phosphorylation of FoxO3a but did not target FoxO1, FoxO4, or FoxO6 for phosphorylation [91]. Conversely, it has been shown that AICAR treatment regulates levels of FoxO1 in hepatic HepG2 cells [92]. Based on all these results, I speculated that both FoxO1 and FoxO3a are subjected to AMPK regulation, at least in muscle cells.

Evidence suggested that a similar relationship might exist between AMPK and myostatin levels. I confirmed in this study that 180EC stimulated myostatin levels and that myostatin levels in L6 cells were induced in an AICAR concentration-dependent manner. As alluded to earlier, Zhang et al. [87] and Chen et al. [86] have demonstrated that myostatin regulates both levels and activity of FoxO proteins. Furthermore, it has been reported that AMPK activation induces myostatin expression in C2C12 cells [88]. From the result where myostatin levels increase in an AICAR concentration-dependent manner suggests that myostatin is regulated as a downstream of AMPK.

In summary, I demonstrated elevated levels of AMPK activation on day 7 after 180EC with ankle joint torque deficits. Furthermore, AMPK activation reduced levels of the phosphorylated forms of FoxO1 and FoxO3a and stimulated myostatin levels, both in a concentration-dependent manner in L6 myotubes. Thus, I conclude that AMPK

activation plays an important role in the regulation of FoxO1, FoxO3a, and myostatin activity, and these results could explain the elevation of total FoxO1, FoxO3a, and myostatin levels in response to 180EC. Additional studies are required to clarify the observation that AMPK is activated on day 7 post-180EC.

Taken together, I consider that 180EC result in both AMPK activation and phosphorylation of AMPKα, whereas 30EC induce only AMPK activation (phosphorylation of ACC).

2-5 Figures

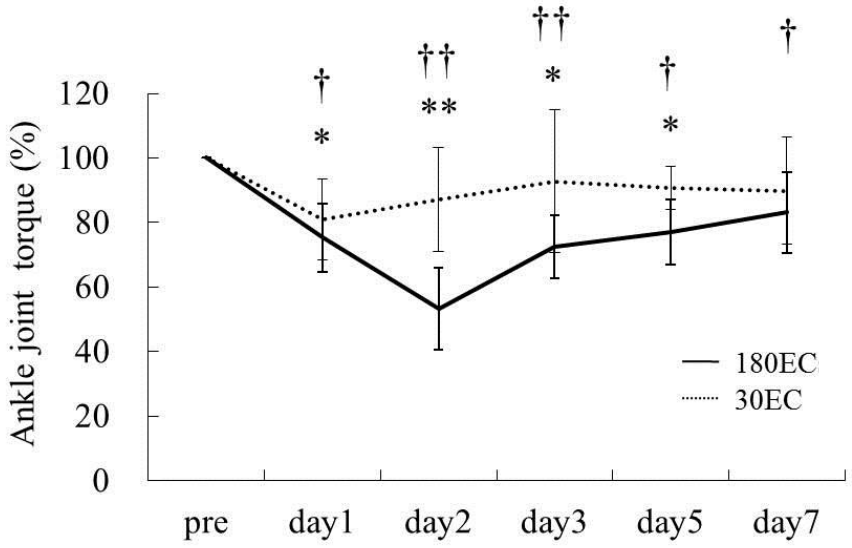

Figure 2-1. Time course changes of rat ankle joint torque after eccentric contractions

180EC: eccentric contractions with 180°/s angular velocity, 30EC: eccentric contractions with 30°/s angular velocity. The values are expressed as mean ± SD. **P* < 0.05, ***P* < 0.01, 180EC vs. 30EC. †*P* < 0.05, ††*P* < 0.01, 180EC vs. pretreatment value.

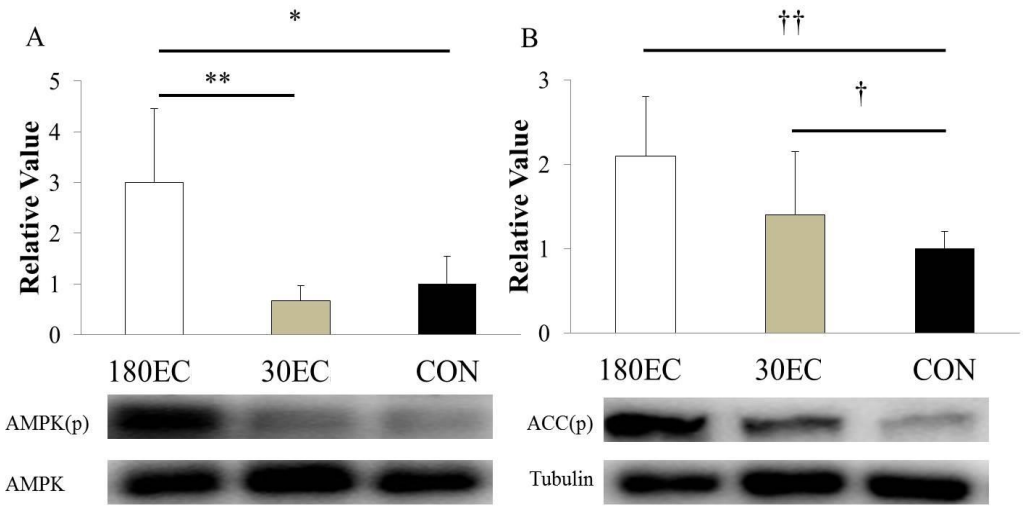

Figure 2-2. Levels of relative phosphorylated AMPK (A) and Phosphorylated ACC (B) on day 7 post-ECs

180EC: eccentric contractions with 180°/s angular velocity, 30EC: eccentric contractions with 30°/s angular velocity, CON: control group. The values are expressed as mean ± SD. (A) **P* < 0.05, ***P* < 0.01, vs. 180EC. (B) †*P* < 0.05, ††*P* < 0.01, vs. CON.

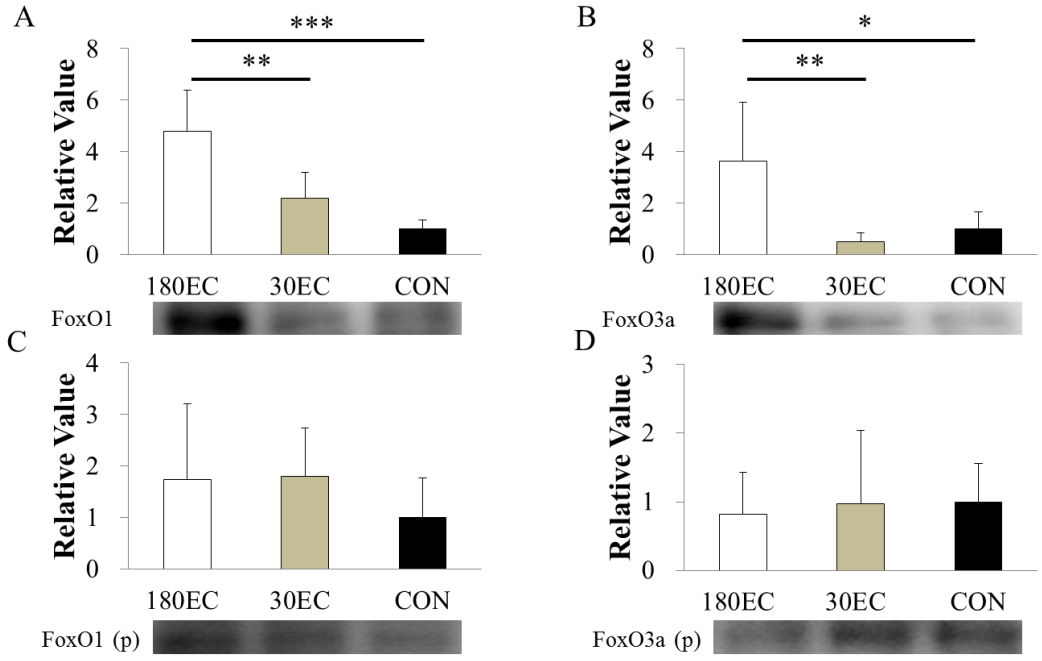

Figure 2-3. Levels of FoxO1(A) and FoxO3a(B) and phosphorylated FoxO1(C) and FoxO3a(D) on day 7 post-ECs

180EC: eccentric contractions with 180°/s angular velocity, 30EC: eccentric contractions with 30°/s angular velocity, CON: control group. The values are expressed as mean ± SD. **P* < 0.05, ***P* < 0.01, ****P* < 0.001, vs. 180EC.

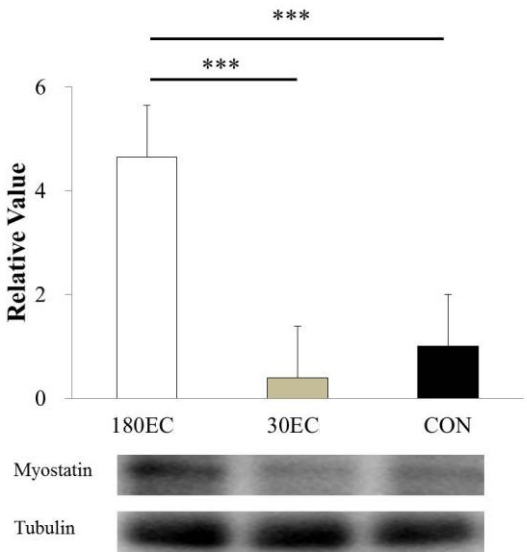

Figure 2-4. Level of myostatin on day 7 post-ECs

180EC: eccentric contractions with 180°/s angular velocity, 30EC: eccentric contractions with 30°/s angular velocity, CON: control group. The values are expressed as mean ± SD.

***$P < 0.001$, vs. 180EC.

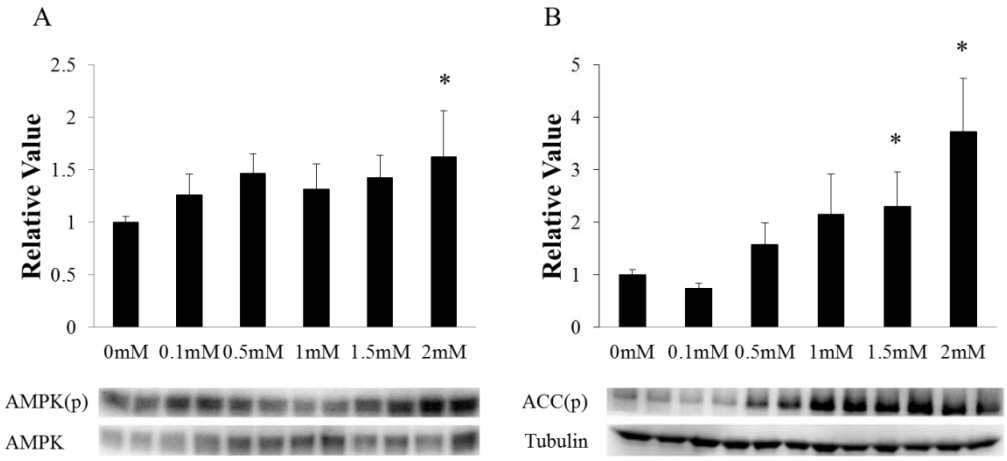

Figure 2-5. Effect of AICAR treatment on phosphorylated AMPK(A) and ACC(B) level in L6 myotubes

L6 myotubes were treated with different concentration (0mM, 0.1mM, 0.5mM, 1mM, 1.5mM, 2mM). The values are expressed as mean ± SD (n = 6). *$P < 0.05$, vs. 0mM.

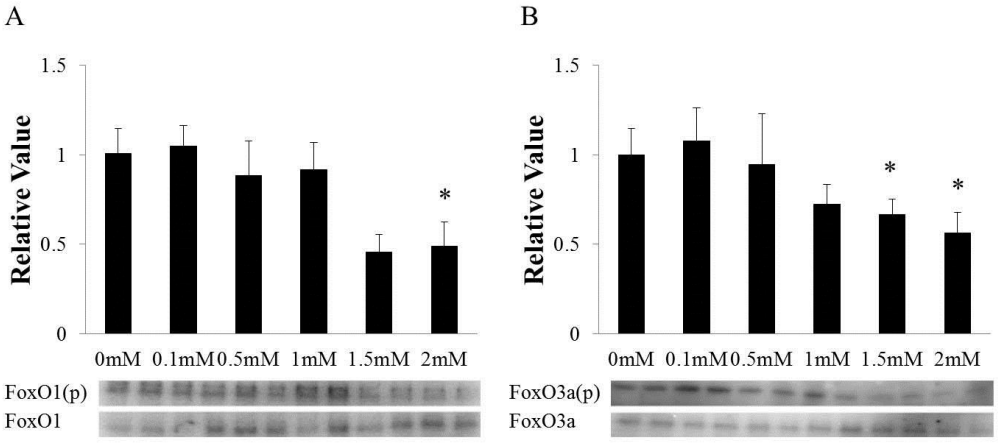

Figure 2-6. Effect of AICAR treatment on phosphorylated FoxO1(A) and FoxO3a(B) to the total level in L6 myotubes

L6 myotubes were treated with different concentration (0mM, 0.1mM, 0.5mM, 1mM, 1.5mM, 2mM). The values are expressed as mean ± SD (n = 6). *$P < 0.05$, vs. 0mM.

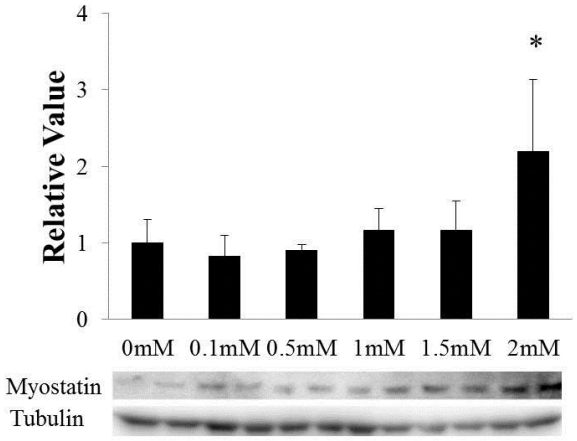

Figure 2-7. Effect of AICAR treatment on myostatin level in L6 myotubes

L6 myotubes were treated with different concentration (0mM, 0.1mM, 0.5mM, 1mM, 1.5mM, 2mM). The values are expressed as mean ± SD (n = 6). *P < 0.05, vs. 0mM.

Chapter 3.

Severe eccentric contractions accompanying muscle injury induce structural damage and functional deficits of the peripheral nerve in rats

3-1 Purpose

The aim of chapter 3 was to investigate whether ECs with fast angular velocities to the gastrocnemius muscle damage the sciatic nerve by measure of NCV and molecular analyses. I hypothesized that gastrocnemius muscle inducing muscle protein degradation by ECs produces structural damage and functional deficits to the sciatic nerve and its branches.

3-2 Materials and Methods

Animal care

Male Wistar rats were purchased from CLEA Japan, Inc. (Tokyo, Japan). Rats (age, 11 weeks; body mass, 285–358 g; n = 66) were assigned randomly to 1 of 3 groups: a 180EC group (180EC; ECs with 180°/s angular velocity; n = 30), a 30EC group (30EC; ECs with 30°/s angular velocity; n = 30), and a control group (CON; n = 6). Rats in the 2 ECs groups were further assigned to day-3-, day-7-, and day-10-subgroups (n = 10 each). The angular velocities in the 180EC and 30EC groups were chosen based on previous studies [25, 93]. All rats were housed in individually ventilated cage systems (Tecniplast S.p.A., Milan, Italy) that were maintained at 22–24°C with a 12:12-h light: dark cycle and they were provided with water and food *ad libitum*. The right hindlimbs of all rats were shaved, and each rat was anesthetized with isoflurane. ECs were induced, and torque and NCV were measured while rats were anesthetized. Three, 7, and 10 days after the ECs, the rats in each group were sacrificed, and the gastrocnemius and soleus were dissected and weighed. The control group did not undergo ECs, but their gastrocnemius and soleus were also dissected and weighed after 7 days with the ECs groups. A portion of the sciatic nerve was excised from the

branching point of the sural nerve to the branching point of medial gastrocnemius nerve, as shown in Figure 1. Experimental procedures were approved by the Ethical Committee for Animal Experiments at the Nippon Sport Science University.

ECs of the gastrocnemius muscle

The ECs system of the gastrocnemius muscle was similar to that used in previous studies [25, 93]. Briefly, before the ECs, anesthetized rats were placed in a prone position on the isokinetic dynamometer. The gastrocnemius muscle of the right hindlimb was stimulated percutaneously with self-adhesive surface electrodes (Vitrode V, Ag/AgCl; Nihon Koden, Tokyo, Japan) connected to an electronic stimulator and an isolator (SS-104J; Nihon Koden, Tokyo, Japan). ECs were induced at 30°/s angular velocity (30EC) or 180°/s angular velocity (180EC) by electrical stimulation of the gastrocnemius muscle with simultaneous forced dorsiflexion of the ankle joint. The forced lengthening contractions ranged from 0° to 45°. Four sets of 5 contractions were induced, with a 5-min interval between each set. The control group was anesthetized only and received no other treatment. In order to confirm a functional deficit, isometric tetanic forces were measured at predetermined times before and after the ECs. Isometric

tetanic torque was measured as reported previously [25]. After the last measurement of isometric tetanic torque, the target muscles (gastrocnemius and soleus) and the sciatic nerve specimens (shown in Figure 3-1) were dissected, weighed, rapidly frozen in liquid N_2, and stored at -80°C until analysis (n = 6 in each group).

NCV

To confirm sciatic nerve damage, NCV was measured with the method reported previously [94-96]. Concisely, the sciatic nerve of the anesthetized rats was exposed. Hook-type stainless-steel electrodes (EKM2-5050, BioResearch center, Tokyo, Japan) were placed at 2 different points on the sciatic nerve (Figure 3-1). The first stimulating electrode (S1) was placed near the branching point of the pudendal nerve, and the second electrode (S2) was placed near the branching point of the tibial nerve. Stimulation was performed with an electronic stimulator (SES-3301, Nihon Kohden Corporation, Tokyo, Japan). M-waves were recorded with a tripolar needle electrode (EKI-2010, Bio Research Center) inserted into the mid-belly of the medial gastrocnemius muscle. The signals were converted digitally with Power Lab/16SP (AD Instruments Japan Inc., Nagoya, Japan).

NCV was analyzed with Power Lab Chart 7 (AD Instruments Japan Inc.) with the data for the latencies of these 2 stimulation points. NCV was calculated as the distance between S1 and S2 divided by the latencies of the waveforms generated by stimulation at the 2 sites. The NCV of the left sciatic nerve served as an internal control for each group. NCV was measured for 4 rats in each group. After measuring NCV, the rats were sacrificed and were not used in further analyses.

Western blotting analysis

The right sciatic nerve branch was homogenized in buffer containing 50 mM Tris HCl (pH 7.4), 150 mM NaCl, 5 mM ethylenediaminetetraacetic acid, 0.5% sodium dodecyl sulfate, 1% deoxycholate, 0.1% Triton X-100, 1% Nonidet P-40, 0.05% mercaptoethanol, 10 mg/mL phenylmethylsulfonyl fluoride, 0.5 mg/mL leupeptin, 0.2 mg/mL aprotinin, and 1 mM Na_3VO_4. The homogenate was centrifuged at 16,000 × *g* for 15 min at 4°C. Protein concentration was determined with a protein concentration determination kit (Protein Assay II; Bio-Rad Laboratories, Inc., Richmond, VA, USA). An aliquot of each sample containing 15 μg of total protein extract was diluted with sample buffer, boiled at 85°C, loaded in the same sodium dodecyl

sulfate-polyacrylamide gel (10% or 12.5%), and separated by electrophoresis. The samples were transferred to polyvinylidene difluoride membranes (ATTO Corporation, Tokyo, Japan), blocked for 1 h with 2% skim milk, and then incubated overnight at 4°C with the following primary antibodies (all diluted 1:1,000): anti-myelin protein zero antibody (rabbit polyclonal ab31851; Abcam plc, Cambridge, UK), anti-gap-43 antibody (rabbit polyclonal antibody H-100; Santa Cruz Biotechnology, Inc., Santa Cruz, CA, USA), anti-TrkC antibody (rat monoclonal antibody MAB1404; R&D Systems, Inc., Minneapolis, MN, USA), anti-rat macrophage antibody (mouse monoclonal antibody T-3003; BMA Biomedicals, Augst, Switzerland), and anti-β-actin antibody (mouse monoclonal antibody 3700s; Cell Signaling Technology, Inc., Danvers, MA, USA). The membranes were then incubated with the secondary antibody for 2 h at room temperature. Horseradish peroxidase-conjugated goat anti-rat immunoglobulin G (IgG), anti-rabbit IgG (dilution, 1:10,000), or anti-mouse IgG (dilution, 1:10,000) was used as the secondary antibody. Chemiluminescent signals were detected with chemiluminescent reagents (SuperSignal West Dura; Thermo Fisher Scientific Inc., Rockford, IL, USA) and scanned with a chemiluminescence detector (AE6961; ATTO Corporation). All data were quantified with a software package (CS Analyzer; ATTO Corporation) and expressed relative to the levels obtained for the control group.

Immunohistochemistry

The harvested sciatic nerve segments were fixed with 4% paraformaldehyde overnight at 4°C and dehydrated in 30% sucrose in 0.1 M phosphate buffer (pH 7.4) for 6 h at 4°. The sciatic nerve segments were then embedded in OCT compound and frozen in liquid N_2. The frozen samples were stored at -80°C. Cross-sections (10-μm in thickness) were cut with a cryostat at -20°C and mounted on glass slides. The glass slides were then washed 3 times for 10 min. In order to block any nonspecific reactions, the sections were blocked for 1 h with 0.1 M phosphate-buffered saline (PBS) containing 1% bovine serum albumin and 0.01% Triton X-100. The sections were then incubated overnight at 4°C with the primary antibodies, including an anti-TrkC antibody (rat monoclonal antibody, diluted 1:300, R&D Systems, Inc.), which were diluted in 0.1 M PBS containing 1% bovine serum albumin and 0.01% Triton X-100. The sections were washed 3 times with 0.1 M PBS and incubated overnight at 4°C with the secondary antibody, Texas red-labeled goat anti-rat IgG (Vector Laboratories, Inc., Burlingame, CA, USA, 1:500), that was diluted in 0.1 M PBS containing 1% bovine serum albumin and 0.01% Triton X-100. The sections were washed 3 times with 0.1 M PBS, rehydrated in 0.1 M PBS containing 0.2% Triton X-100 for 20 min at room temperature, and stained with Fluorescent Myelin Stains (1:300, Green Fluorescent

Myelin Stains, F 34651) that were diluted in 0.1 M PBS containing 0.2% Triton X-100 for 20 min at room temperature. After the staining was complete, the solution was removed, and the sections were washed 3 times with 0.1 M PBS for 10 min. The sections were coverslipped with mounting medium containing 4′,6-diamidino-2-phenylindole (Vectashield, Vector Laboratories, Inc.) and viewed with a florescence microscope (Olympus model BX 60; Olympus Corporation, Tokyo, Japan). The images were captured with a digital camera (Olympus model DP 70; Olympus Corporation) and analyzed with Olympus DP 70 controller software.

Statistical analysis

Two-way ANOVA was used to compare the body mass, the muscle wet weights, the changes in isometric tetanic torque over time, NCVs, and protein expression levels. *Post hoc* tests were performed by Bonferroni tests. All values are expressed as mean ± standard deviation. *P* values less than 0.05 were considered statistically significant.

3-3 Results

Physiological change in gastrocnemius muscle and sciatic nerve after ECs

After the ECs, no significant differences in the wet weights of the soleus muscles were observed among the 3 groups. However, the wet weights of the gastrocnemius muscles in the 180EC group were significantly increased on day 3 (4.99 mg/ gram body weight) compared to those on day 10 (4.61 mg/ gram body weight) ($P < 0.05$) (Table 3-1).

Isometric tetanic torque was measured after the ECs. The isometric tetanic torque of the 180EC group remained significantly lower than that of the 30EC group until day 7 after the ECs (day 7, $P < 0.05$; day 1, day 2, day 3, and day 5, $P < 0.01$) (Figure 3-2). Moreover, significant torque deficits relative to the pretreatment values were observed in the 180EC group from days 1 to 5 after the ECs (day 1, day 3, and day 5, $P < 0.01$) (Figure 3-2). In contrast, no torque deficits were observed in the 30EC group.

In order to examine the functional nerve damage caused by the ECs, the NCVs were examined. NCVs in the 180EC group on day 7 after the ECs were significantly lower than those in the control group ($P < 0.05$) (Figure 3-3A). No significant

differences were observed between the 30EC groups and the 180EC groups (Figure 3-3B).

Change in molecular expressions of gastrocnemius muscle and sciatic nerve after ECs

The levels of myelin sheath protein zero (p0) which decreases when the myelin sheath is damaged were examined.[67, 97] On day 7 after the ECs, the p0 content was significantly lower in the 180EC group than in the 30EC group ($P < 0.05$) (Figure 3-4A). In addition, the p0 content differed significantly between the day-3 and day-7 180EC groups ($P < 0.05$) (Figure 3-4A). In contrast, the p0 content in the 30EC group remained almost the same after the ECs. No significant differences between the GAP-43 contents were observed (Figure 3-4B).

The levels of the macrophage related protein (ED1) after the ECs were measured. The ED1 levels of the 180EC group were significantly higher on day 7 than on day 3 ($P < 0.05$) (Figure 3-4C). Significantly higher ED1 levels in the 180EC groups were also observed in comparison with the levels of the 30EC group on day 7 after the ECs ($P < 0.01$) (Figure 3-4C).

TrkC levels in the 180EC group were significantly higher on day 7 than on day 3 or day 10 ($P < 0.01$) (Figure 3-4D). TrkC levels on day 7 were also significantly higher in the 180EC group than in the 30EC group ($P < 0.05$) (Figure 3-4D). In addition, localization of TrkC was observed by immunohistochemistry. Immunoreactive signals of TrkC were detected in the myelin sheath, suggesting that TrkC localized Schwann cells around myelin. Strong TrkC signals were observed only in the 180EC group on day 7 after the ECs (Figure 3-5).

3-4 Discussion

The significant decrease in NCVs and p0 levels on day 7 only in the 180EC suggests that the myelin sheath was damaged by ECs with a 180°/s angular velocity. Using ED1 as a marker for rat macrophages when sciatic nerve is damaged [98], the significant increases in ED1 levels in the 180EC group would be consistent with an inflammatory reaction in the sciatic nerve and its branches innervating the ECs-damaged gastrocnemius muscle. The increase in TrkC levels in the 180EC group suggests that reconstruction of the nerve cells occurred.

The greater wet weight of the gastrocnemius in the 180EC group on day 3 than on day 10 appears to be due to increased inflammation and swelling, based on the development of ultrastructural collapse, edema, and inflammation of myofibers [14, 99]. These lines of evidence suggest that muscles are seriously damaged on days 2–3 after ECs. Although several groups have reported that fast ECs velocities do not result in increased damage [100, 101], my data suggest that ECs with faster angular velocity (180°/sec) seriously damaged the gastrocnemius muscles, compared with slow angular velocity (30°/sec).

Reductions in NCVs by diabetes and neurogenic diseases have been reported [102,

103]. Although muscle damage induced by ECs has not been reported to produce reductions in NCV, several reports suggest that ECs damage both muscle and nerve cells. Functional damage to the sciatic nerve by vigorous ECs is supported by the reduced NCVs of the 180EC group on day 7 after the ECs, in contrast to results in the 30EC group.

I examined the molecular alterations of the sciatic nerve branch and found that the amount of p0 in the 180EC group was lower on day 7 than on days 3 or 10. The myelin sheath consists of p0, MAG, and PMP22, and when the nerve is damaged, the levels of these proteins decrease [67, 97]. Although future studies should further evaluate MAG and PMP22 levels, the results that were obtained for p0 indicated that the myelin sheath was damaged after the 180EC. In addition, I showed that levels of a macrophage-related protein in the 180EC group on day 7 were greater than those in the 180EC group on day 3 or the 30EC group on day 7. If the myelin sheath is damaged, macrophages increase in number in the damaged area of nerve cells [60, 62, 64, 65]. After re-myelination is complete, the macrophage numbers also return to baseline levels. Axon regeneration is characterized by formation of a growth cone. GAP-43 is expressed at high levels in neuronal growth cones during development and axonal regeneration [104]. On day 7 after the 180EC, p0 decreased, while GAP-43 did not differ

significantly among all groups. The same tendency was not observed in the 30EC groups. Taken together, these results suggest that the myelin sheath, but not the axon, was damaged after the detrimental ECs, as has been shown in neuropraxia [2]. From the results of the functional and molecular examinations, we conclude that the injury in the nerve cells was prominent on day 7 after the ECs.

The NCV reductions and myelin sheath damage in the 180EC group were observed on day 7, suggesting that there was a delay between the ECs and nerve injury. Although we examined the sciatic nerve branch, I believe the ECs initially damaged motor unit, neuromuscular junctions and intramuscular nerve, as has been reported by others [57, 58, 71]. Kami et al. have reported that gastrocnemius contusion injuries induced intramuscular axonal damage with retrograde propagation to the cell body in the spinal cord [59]. They have shown that apparent damage in motor neurons and intramuscular nerves were observed 3 days after the muscle injury [59]. Furthermore, in cases of nerve crush injury, the sciatic function index and myelin thickness in damaged nerve have been shown to be affected 7 days after crush treatment [105, 106]. I think that the damage to nerve cells was initiated in the skeletal muscle, and it was then transmitted in a retrograde direction to the innervating nerves. These are time-consuming events. In addition, I found that disorders in the nerve cells occurred in

only the 180 EC groups, suggesting that strong eccentric contractions induced nerve damage.

Schwann cell migration and proliferation provide an essential supportive function for the myelin sheath [68]. Schwann cells are also involved in many important aspects of peripheral nerve development and regeneration [4, 5]. NT-3 and TrkC are involved in Schwann cell migration [61]. In this study, I showed that the expression levels of TrkC in the 180EC group on day 7 were higher than those in the 180EC group on days 3 or 10 or in the 30EC group on day 7. The 3 most common types of Trk receptors are TrkA, TrkB, and TrkC. Each of these receptor types has different binding affinities for certain types of neurotrophins. TrkC is ordinarily activated by binding NT-3. Because the activation of TrkC by NT-3 induces Schwann cell migration, higher levels of TrkC suggest that the damaged myelin sheath is being repaired by Schwann cells. I confirmed that TrkC expression was localized to Schwann cells around the myelin sheath, suggesting that Schwann cells were activated by TrkC after 180°/s ECs. BDNF activation of the p75 NTR is also involved in Schwann cell proliferation. The differences in the signaling pathways initiated by these distinct types of receptors are important for generating diverse biological responses. In addition, p75 NTR enhances myelination by binding to BDNF during neuronal regeneration [67, 68]. The

orchestration of these signaling molecules in nerve injuries that are induced by ECs should be examined further.

Damage to the myelin sheath may reduce NCV and possibly cause muscle atrophy [106, 107]. Although we found reductions in NCVs, I did not observe decreased wet weights of examined muscles. However, Ochi et al. have reported that ECs with 180°/s angular velocities induce higher expression levels of FoxO1 and FoxO3a [25]. Furthermore, they observed that 30EC did not induce the expression of FoxO proteins. As FoxO proteins lead to degradation of muscle proteins, muscles subjected to 180°/s ECs might atrophy. This catabolic process might be initiated by neural tissue damage.

Because I used anesthetized animals, electrical stimulation, and a larger range of motion, factors other than ECs might have induced the neural tissue damage. In order to exclude these possibilities, I confirmed that the 30EC group did not show any indications of neural tissue damage, and thus concluded that a 180°/s angular velocity and resultant force deficits were key to the induction of neural tissue damage by ECs.

I showed that ECs of the gastrocnemius muscle induce damage of the myelin sheath and cause reduction of NCVs, consistent with damage to nerve cells. I suspect that the damaged nerve might in turn exacerbate injured muscle, a concept which may

lead to novel ideas for prevention and treatment of ECs-induced muscle injury. Because it is not clear whether this animal model is relevant to injuries induced by voluntary action, future studies should assess whether voluntary ECs-related exercise affects the function of human nerve.

In the study of chapter 3, I observed damage of the sciatic nerve on day 7 post-180EC in rat gastrocnemius muscle [108]. Probably, sciatic nerve damage activates AMPK and activated AMPK induces protein degradation. Even if this is the case, this conclusion is well matched with the previous study showing [109] that AMPK activation with AICAR failed to prevent protein degradation in denervated gastrocnemius and soleus muscle. Although nerve crush injury has been found to induce elevated myostatin, AMPK activation has not been observed in response to nerve crush injury [75]. Therefore, in the chapter 4, I researched to determine whether protein degradation by nerve crush injury induces AMPK activation.

3-5 Table and Figures

		Day 3		Day 7		Day 10	
	CON	30EC	180EC	30EC	180EC	30EC	180EC
BW (g)	326.9 ± 6.58	321.3 ± 7.45	311.1 ± 16.87	342.1 ± 9.57	330.7 ± 8.46	347.8 ± 15.51	345.0 ± 4 .27
Sol/BW (mg/g)	0.395 ± 0.02	0.372 ± 0.03	0.379 ± 0.02	0.369 ± 0.03	0.398 ± 0.01	0.391 ± 0.02	0.333 ± 0.02
Sol(mg)	129.4 ± 9.49	119.7 ± 9.03	117.7 ± 5.72	126.2 ± 10.19	131.9 ± 3.89	136.0 ± 7.23	115.2 ± 10.29
Gas/BW (mg/g)	4.665 ± 0.09	4.860 ± 0.14	4.995 ± 0.35 *	4.740 ± 0.08	4.935 ± 0.11	4.872 ± 0.10	4.619 ± 0.23 *
Gas (mg)	1525.8 ± 55.90	1561.5 ± 43.16	1550.8 ± 83.24	1621.8 ± 39.83	1631.9 ± 34.82	1694.7 ± 87.30	1594.0 ± 97.34

Table 3-1. Body weight and wet weight of soleus and gastrocnemius after ECs

CON: the control group, 30EC: ECs with 30°/s angular velocity, 180EC: ECs with 180°/s angular velocity. BW: body weight, Sol: soleus, Gas: gastrocnemius. Values are expressed as the mean ± SD. *: $P < 0.05$ between groups.

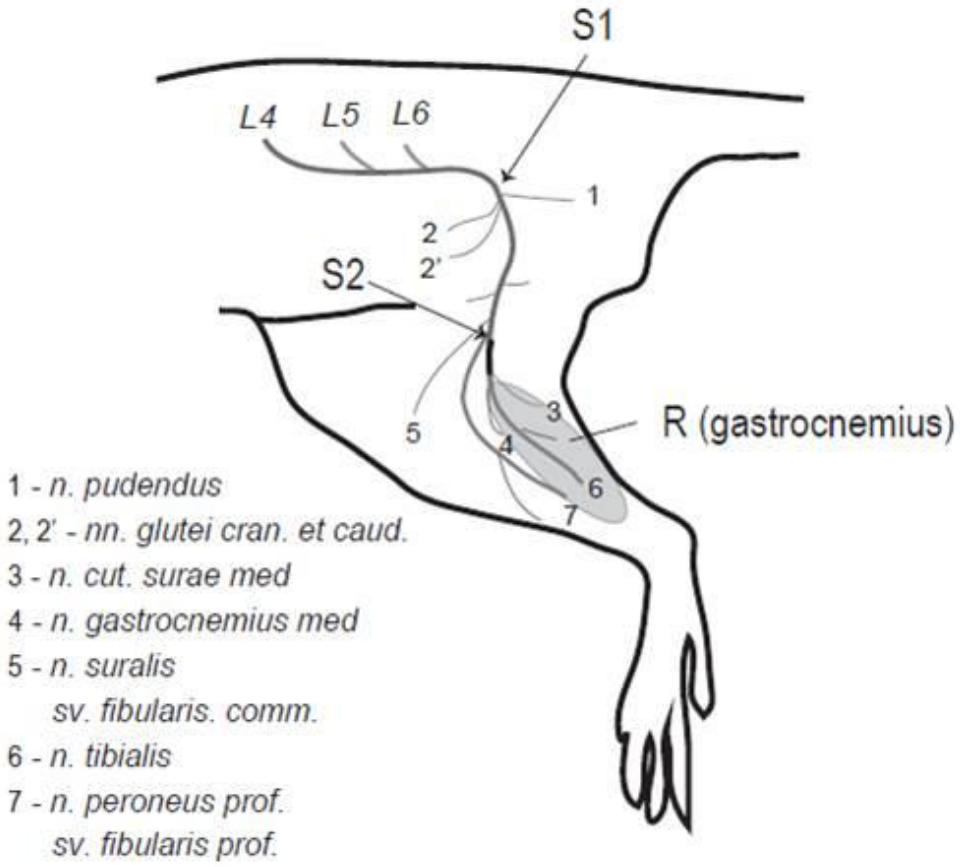

Figure 3-1. Schematic representation of the sciatic nerve and its branches

S1 (proximal): the branching point of pudendus nerve, S2 (distal): the branching point of tibialis nerve. Induced M-wave was taken at the mid-belly of medial gastrocnemius muscle (R). The black line of the sciatic nerve branch shows the tissue that was excised for western blotting and immunohistochemistry.

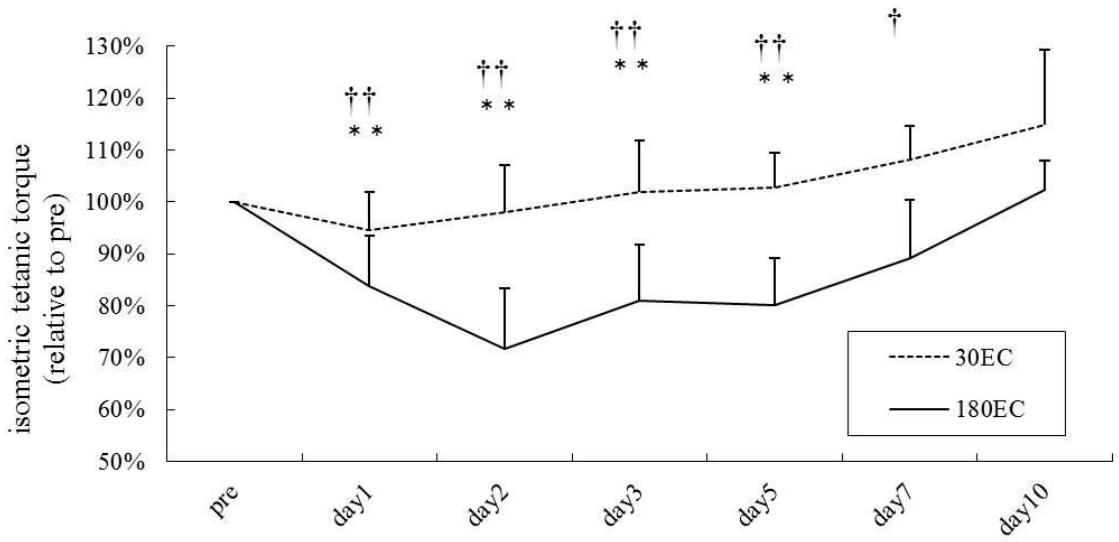

Figure 3-2. Time course changes in isometric tetanic torque after ECs

The isometric tetanic torque in the 180EC group was decreased significantly compared with that of the 30EC group and the pretreatment values. 30EC: ECs with 30°/s angular velocity, 180EC: ECs with 180°/s angular velocity. Statistical significance:*P<0.05, **P<0.01 180EC vs. pretreatment value; †P<0.05, ††P<0.01, 180EC vs. 30EC.

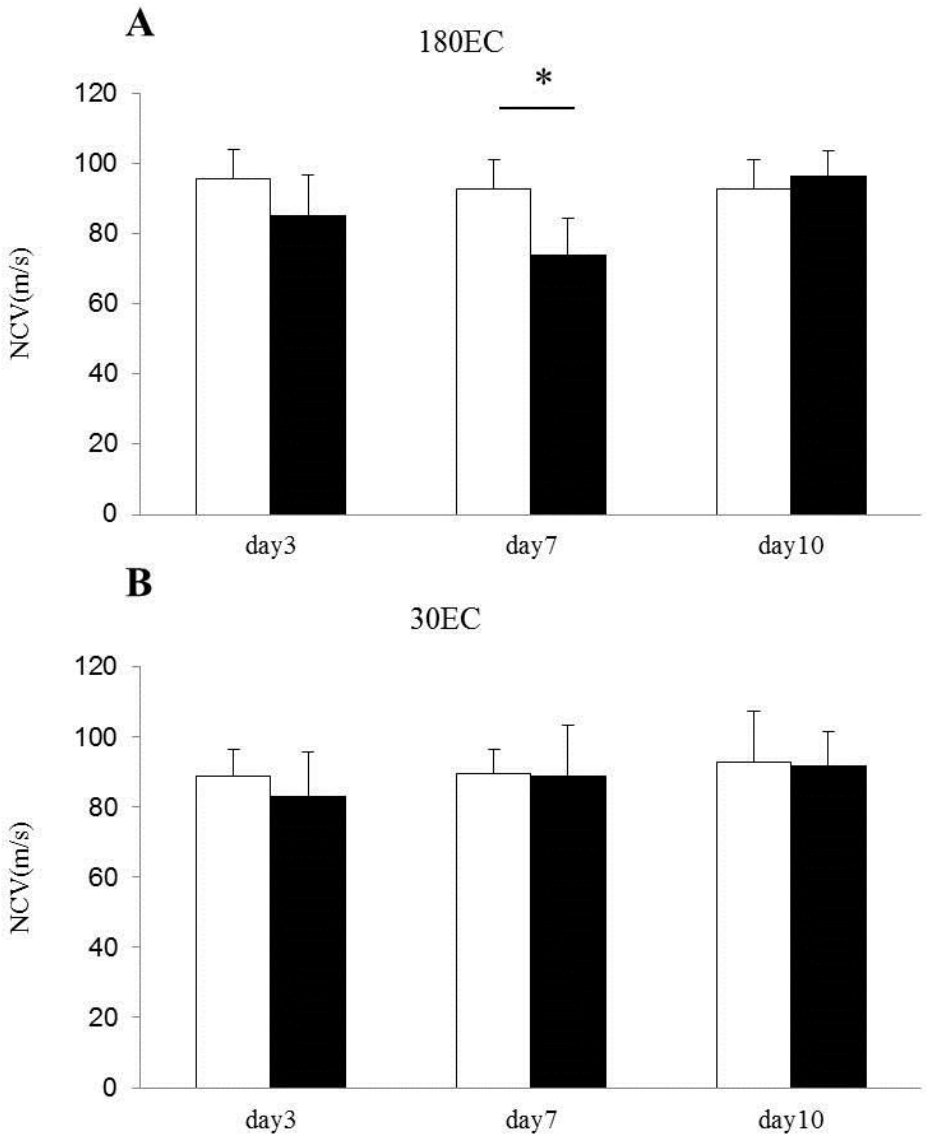

Figure 3-3. Nerve conduction velocities after ECs

(A) The NCV in the day-7 180EC group was decreased significantly compared with the control group. (B) NCVs in the 30EC groups were not decreased compared with the control groups. Open bars, internal control for each group; Black bars, ECs groups.30EC: ECs with 30°/s angular velocity; 180EC: ECs with 180°/s angular velocity. Statistical significance: *P<0.05, 180EC vs. CON.

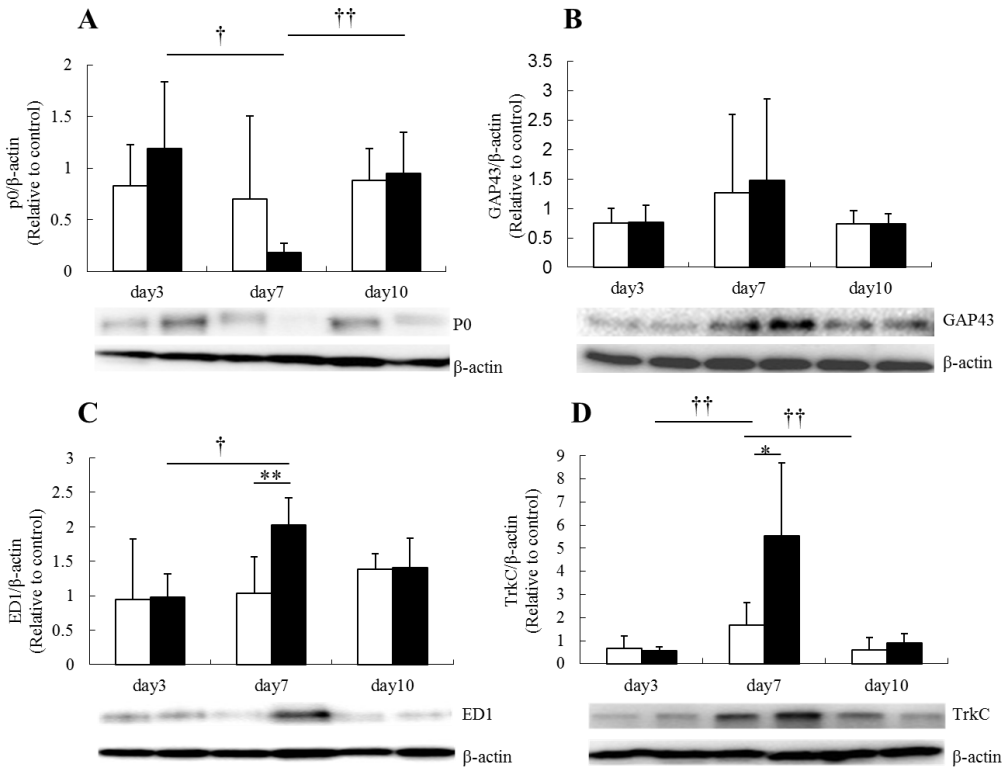

Figure 3-4. Contents of p0, GAP-43, ED1, and TrkC after ECs

(A) Contents of p0 after ECs. The amount of p0 in the 180EC group was significantly lower on day 7 than on days 3 or 10. (B) Contents of GAP-43 after ECs. No significant changes were observed among the groups. (C) Invasion of macrophages into nerve tissue after ECs. (D) Immunoblotting for TrkC. 30EC: ECs with 30°/s angular velocity, 180EC: ECs with 180°/s angular velocity. Open bars, 30EC groups; Black bars, 180EC groups. Statistical significance: *P<0.05, **P<0.01, 180EC vs. 30EC; †P<0.05, ††P<0.01, 180EC day7 vs. 180EC day3 or day10.

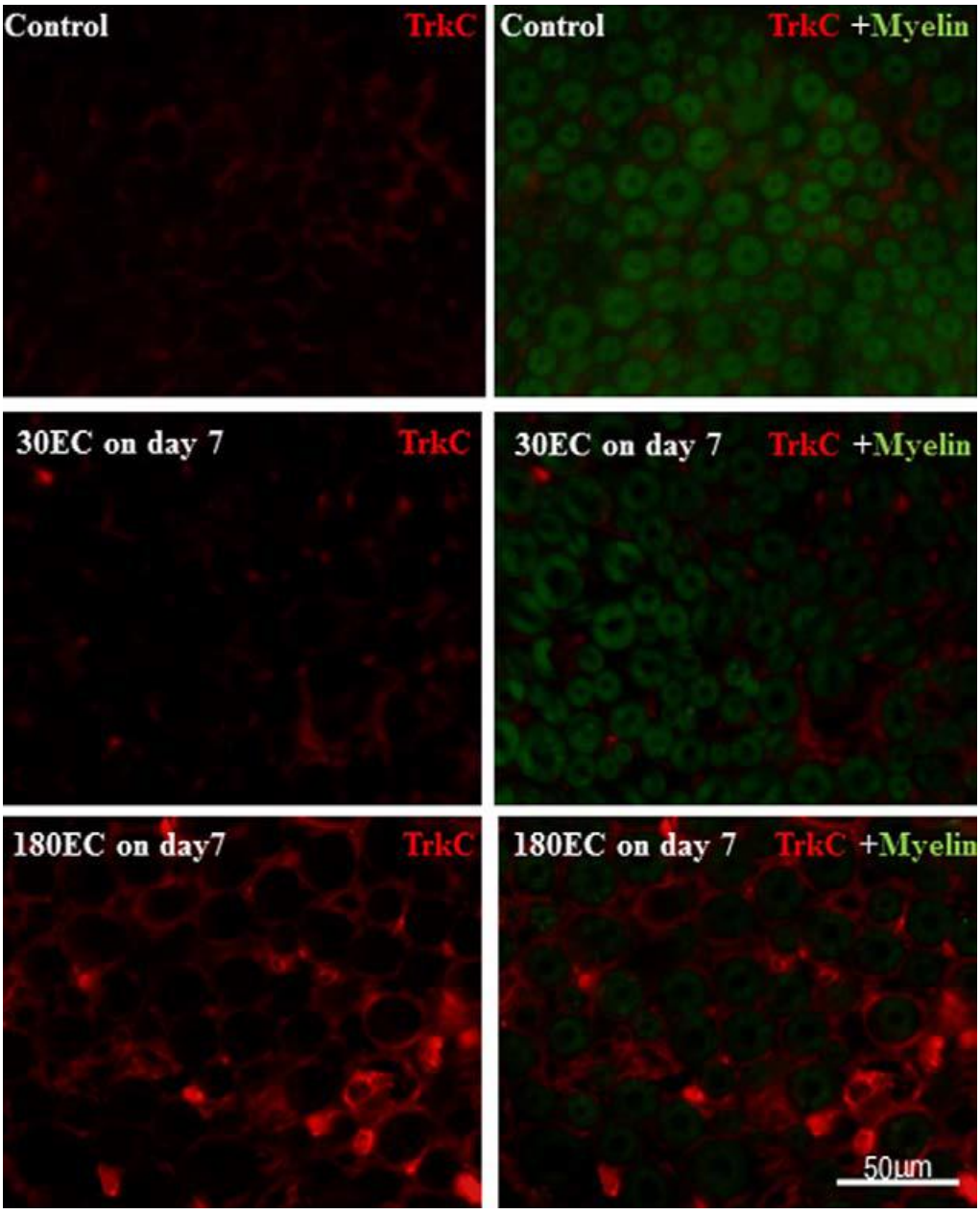

Figure 3-5. Immunohistochemistry of TrkC after ECs

A strong TrkC signal relative to the 30EC group on day 7 was observed only in the 180EC group on day 7 after the ECs.180EC: ECs with 180°/s angular velocity, 30EC: ECs with 30°/s angular velocity.

Chapter 4.

Expressions of myostatin and MuRF1 have important roles on muscle protein degradation by nerve crush injury in rats

4-1 Purpose

The object of chapter 4 was to identify whether AMPK activation occurs in muscle atrophy induced by the nerve crush injury (NCI). I hypothesized that AMPK activation stimulates the expression of muscle protein degradation-related factors like in chapter 2. Levels of phosphorylated AMPK and phospho-acetyl CoA carboxylase, and expression levels of FoxO1, FoxO3a, and myostatin were verified to elucidate relationship between AMPK activation and muscle protein degradation after NCI. Furthermore, these results support the hypothesis that nerve damage induced by ECs as shown in the chapter 3, is the cause for AMPK activation induced muscle protein degradation as seen in chapter 2.

4-2 Materials and Methods

Animal care

Male Wistar rats (age, 6 weeks; body mass, 260–280 g; n = 30) were randomly assigned to the following two groups: control group (sham operation group; n = 6) and nerve crush injury group (NCI, n = 24). Furthermore, NCI groups were divided into four groups for analysis of time course. The rats were individually housed in ventilated cage (IVC) systems (Tecniplast, Milan, Italy) maintained at 22–24°C with a 12-h light/dark cycle. Rats were provided water and food ad libitum. At 3 day, 7 day, 14 and 28 day after NCI, 6 rats in each group were dissected and weighed. This study was approved by the Ethical Committee for Animal Experiments at the Nippon Sport Science University.

Surgical procedures of nerve crush injury

NCI was conducted according to the previous reported study [75]. Briefly, the

right hind limbs of all the rats were shaved, and then each rat was anesthetized with isoflurane. (aspiration rate, 450 mL/min; concentration, 2.0%). The right sciatic nerve was exposed through an incision of the right hind leg and was crushed using a forcep clamping for 30 seconds. Left hind leg was left intact. Only incision of the skin was made in the sham-operated control group. After NCI, the incision of right hind leg was stitched and rats were returned to their cages. On days 3, 7, 14 and 28 after surgery, each group was dissected, weighed, immediately frozen in liquid N_2, and stored at –80°C until analysis.

Western blotting analysis

The medial gastrocnemius muscle was macerated in liquid N_2 and homogenized using a RIPA buffer (Pierce, Rockford, USA). The homogenate was centrifuged at 16,000 ×g for 15 min at 4°C. Protein concentrations were determined using a protein concentration determination kit (Protein Assay II; Bio-Rad, Richmond, VA). A 30-μg

(rat samples) total protein extracts from each sample were mixed with sample buffer, boiled, loaded on the same SDS-polyacrylamide gel (5, 10, or 12.5%). The samples were electrophoretically separated and separated proteins were then transferred onto nitrocellulose membranes (GE healthcare, Whatman, Germany). The membranes were blocked for 1 h with tris-buffered saline (TBS) containing 1% triton X and 5% skimmed milk and then incubated overnight at 4°C with the following primary antibodies (dilution, 1:1000): anti-AMPK alpha (#2532; Cell Signaling Technology), anti-p-AMPK alpha (Thr172) (#2535S; Cell Signaling Technology), anti-p-Acetyl-CoA Carboxylase (Ser79) (#3661S, Cell Signaling Technology), anti-FoxO1 (#9454S; Cell Signaling Technology), anti-p-FoxO1(Ser256) (#9461S; Cell Signaling Technology), anti-FoxO3 (#2497S; Cell Signaling Technology), anti-p-FoxO3(Ser253) (#9466S; Cell Signaling Technology), anti-GDF8 (sc-6884; Santacruz Biothechnology), anti-MuRF1(sc-32920; Santacruz Biothechnology), and anti-MAFbx (sc-33782; Santacruz Biothechnology). The membranes were then washed three times and incubated with the secondary

antibody at room temperature. Horseradish peroxidase (HRP)-conjugated goat anti-mouse immunoglobulin G (IgG) or anti-rabbit IgG (dilution, 1:10,000) was used as the secondary antibody. Chemiluminescent reagents were used for detecting the secondary antibody (SuperSignal West Dura; Pierce Protein Research Products, Rockford, IL). Chemiluminescent signals were detected using a chemiluminescence detector (AE9100N; ATTO) and quantified using a personal computer with image analysis software (CS Analyzer; ATTO). The band densities were expressed relative to those obtained for the control.

Statistical analysis

All values are expressed as mean ± standard deviations. One-way analysis of variance (ANOVA) followed by the Fisher exact test was used to compare the body mass, wet weight of gastrocnemius muscle, and expression of protein levels using a micro soft office excel. The significance level was set at $P < 0.05$.

4-3 Results

Body mass and wet weight of gastrocnemius muscle following NCI

Following the NCI, no significant differences in the body mass (Table 4-1) were observed among the each group. However, the wet weights of the right gastrocnemius muscles in the NCI group were significantly decreased until 28 days compared to control group after NCI. The wet weights of the right gastrocnemius muscles were gradually decreased and the group after NCI on day 14 was the lowest among all time points (Figure 4-1).

Relationship between AMPK activation and muscle protein degradation in gastrocnemius muscle

After NCI, AMPK activation was observed using levels of phosphorylated AMPKα and ACC. Although no significant difference in the levels of phosphorylated AMPKα was observed among each group on day 14 after NCI, the level of phosphorylated ACC was significantly higher than control group (Figure 4-2A and 4-2B).

Effects of NCI on muscle protein degradation in gastrocnemius muscle

In order to confirm the molecular mechanism of muscle protein degradation, the expression of FoxO1, FoxO3a, MAFbx, MuRF1 and myostatin was measured using a western blot analysis. As a result, the expression of myostatin gradually increased from on day 3 to day 28. The level of myostatin on day 14 after NCI was significantly higher compare to control group (Figure 4-3A). Similarly, myostatin receptor, Activin type II receptor (ActRIIb) was significantly higher compared to control group on day 14 after NCI (Figure 4-3B). Moreover, the expression of MuRF1 on day 3 after NCI was significantly higher than control group (Figure 4-4A). However, the expression of MAFbx was not significantly different among all time course of NCI (Figure 4-4B). Contrary to the skeletal muscle atrophy by NCI, the muscle protein degradation-related factor, FoxO1 was phosphorylated on day14 after NCI (Figure 4-5A). The phosphorylation of FoxO3a showed no significant differences among all time course of NCI (Figure 4-5B).

4-4 Discussion

In the chapter 2 and 3, I found that higher expressions and/or activated phosphorylation states of FoxO1, FoxO3a, myostatin and AMPK were induced in response to severe (180°/s angular velocity) eccentric contractions accompanying with muscle and nerve damage. In this chapter, I showed that NCI stimulates levels of phosphorylated ACC on day 14 after NCI, as well as the elevated expression of myostatin likely in chapter 2. Furthermore, NCI increases the expression of MuRF1 on day 3 and on day 14 after NCI. On the contrary, levels of phosphorylated FoxO1 and FoxO3a on day 14 after NCI were significantly increased compare to control group.

Since many studies have suggested that regulation of skeletal muscle AMPKα1 and α2 differs depending on exercise intensity [79-82], no phosphorylated AMPKα but phosphorylated ACC could be supposed that different AMPK isotype would phosphorylate ACC. Especially in NCI, a consumption of ATP might be induced not by exercise but by regeneration of damaged muscle and nerve. The fashion of ATP consumption in regeneration process might differ from the situation in eccentric contraction exercise. In addition, I suspect whether AMPK activity always associate with phosphorylated states of ACC. Taken together, even though higher level of phosphorylated ACC was observed after NCI, another molecular mechanism, except

for AMPK alpha would play a role in this phenomenon.

I observed that NCI regulates expression of strong atrophy-related factor, myostatin. As a previous study [75], our experimental model of ECs stimulates the expression of myostatin. Since high expression of myostatin has been reported on day 14 after NCI in rat gastrocnemius muscle [75] by others, increased level of myostatin shown in this chapter is likely to a result of NCI. Probably, the sciatic nerve damage activates the expression of myostatin and up-regulates myostatin which might induce the muscle protein degradation. Although AMPK activation was only confirmed by ACC phosphorylation states after NCI treatment, expression of myostatin is undoubtedly induced by NCI.

In this study, elevated expression of MuRF-1 was confirmed on day 3 and day 14 after NCI. In previous studies of sciatic nerve dissection (usually stated as muscle denervation), it has been reported that the expression of MuRF-1 was induced during early stage (at 3 days) after muscle denervation [110]. Therefore, I have speculated that the increase of MuRF-1 appears in an early stage (at 3 days) and again up-regulated in a late stage (at 14 days) after NCI. I speculate that elevation of myostatin on day 14 after NCI might stimulate expression of MuRF-1 and, as a result, muscle atrophy reached its peak on day 14 after NCI.

Even though NCI elevated the expression of myostain and MuRF-1, FoxO1 and FoxO3a were phosphorylated. Since phosphorylated FoxO1 and FoxO3a mean suppress of muscle protein degradation, these results oppose with the results of myostatin and MuRF-1. However, one group reported that denervation atrophy is independent on Akt and mTOR activation and is not rescued by myostatin inhibition [111]. Moreover, they confirmed that phosphorylated FoxO3a did not change after denervation. Therefore, their results and my results are similar in the way that muscle protein degradation following nerve damages was not affected by the levels of FoxOs.

In conclusion, I examined the possibility that elevated level of AMPK activation induces the expression of myostatin with muscle atrophy and nerve damage on day 14 after NCI. As a result, I failed to confirm time course association of AMPK activation with the phosphorylated FoxO1 and FoxO3a. Thus, I conclude that the role of AMPK-FoxO axis is not so apparent in NCI induced muscle atrophy. With regard to myostatin and MuRF1, elevated expressions were observed on day 14, suggesting that myostatin induced muscle protein degradation is important in NCI induced muscle atrophy.

4-5 Table and Figures

	CON	Day 3	Day 7	Day 14	Day 28
BW (g)	283.11 ± 9.96	266.1 ± 17.16	280.3 ± 22.02	284.98 ±7.98	314.88 ± 9.30
Gas/BW (mg/g)	4.60 ± 0.16	3.92 ± 0.20 **	3.26± 0.58 **	2.69 ± 0.59 **	3.82 ± 0.23 **
Gas (mg)	1302.01 ± 44.35	1046.53± 12.03	917.53 ± 19.77	768.81 ± 15.52	1205.16± 77.26

Table 4-1. Body weight and wet weight of gastrocnemius after NCI

CON: the control group, BW: body weight, Gas: gastrocnemius. The values are expressed as mean + SD.

***P* < 0.01, vs. CON. Post hoc tests were performed by Fisher exact test

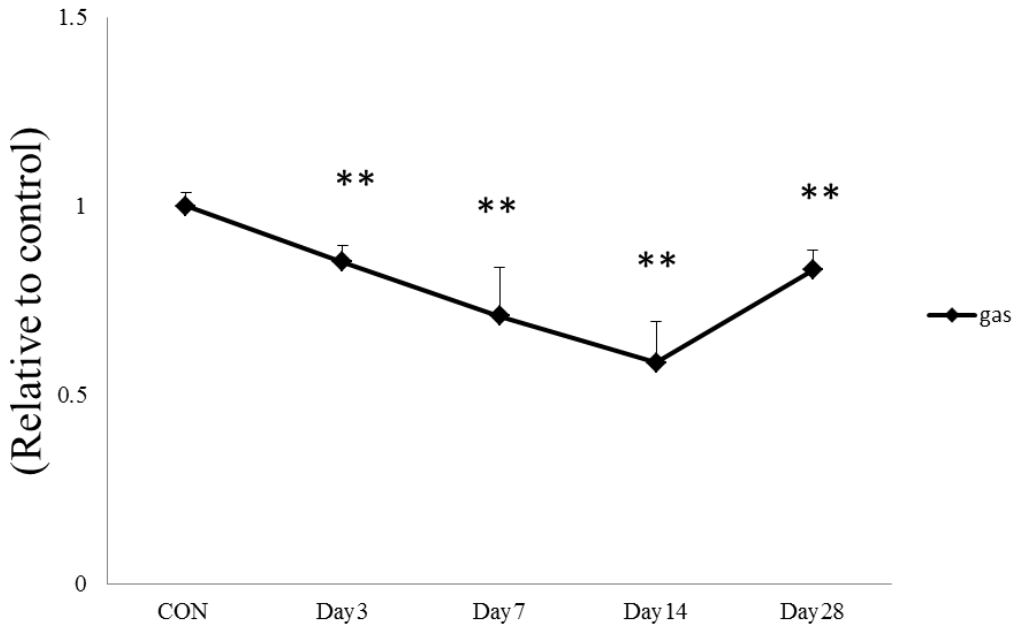

Figure 4-1. The time course change in wet weight of gastrocnemius muscle (gas) after NCI

The values are expressed as mean + SD. *P < 0.05, **P < 0.01, vs. CON.

Post hoc tests were performed by Fisher exact test

A

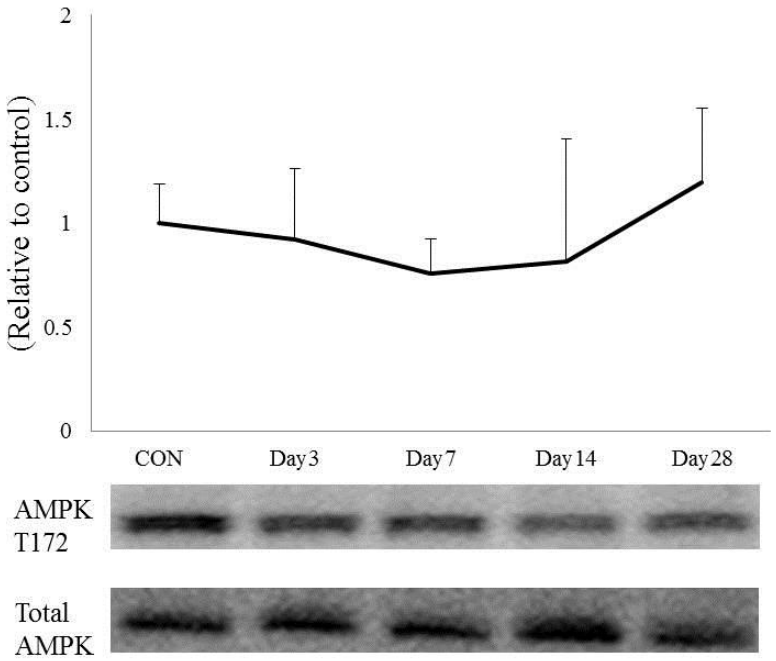

Figure 4-2A. Level of phosphorylated AMPK until 28 day post-NCI

The values are expressed as mean + SD.

B

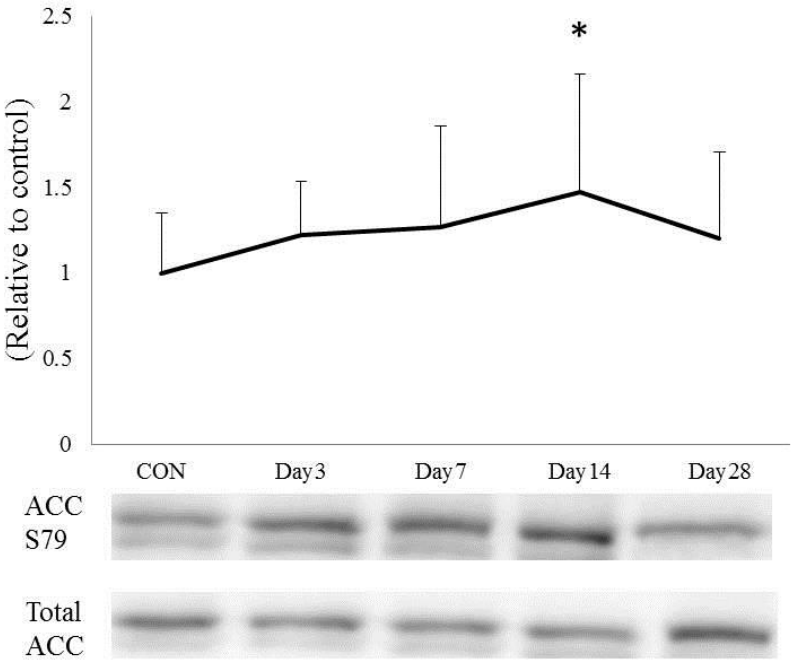

Figure 4-2B. Level of phosphorylated ACC until 28 day post-NCI

The values are expressed as mean + SD.

*P < 0.05, vs. CON. Post hoc tests were performed by Fisher exact test

A

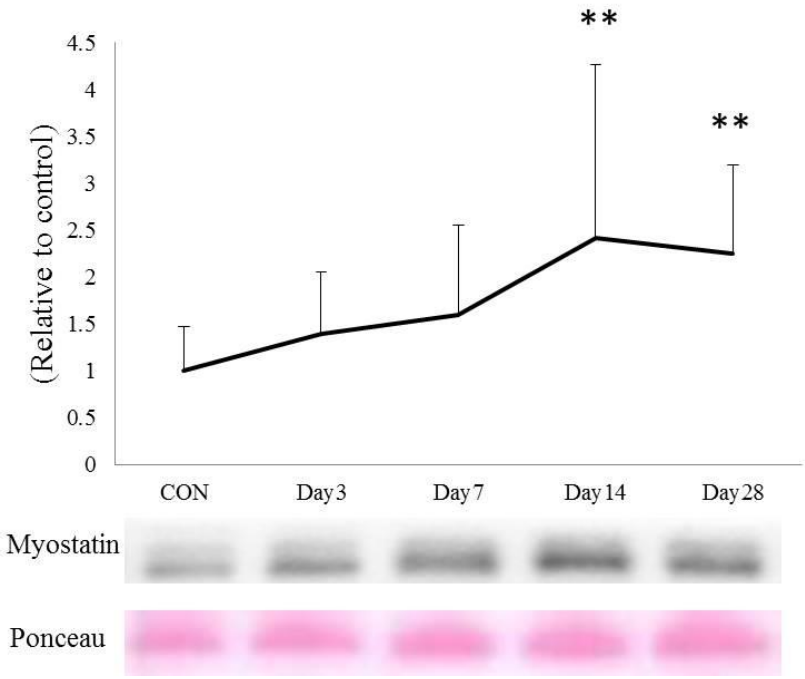

Figure 4-3A. The expression of myostatin until 28 day post-NCI

The values are expressed as mean + SD.

***P* < 0.01, vs. CON. Post hoc tests were performed by Fisher exact test

B

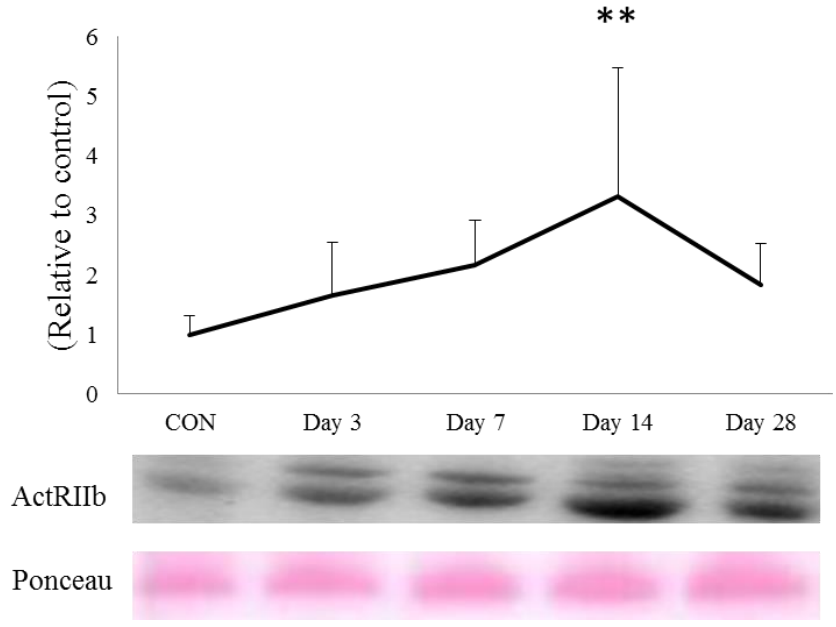

Figure 4-3B. Level of ActRIIb until 28 day post-NCI

The values are expressed as mean + SD.

***P* < 0.01, vs. CON. Post hoc tests were performed by Fisher exact test

A

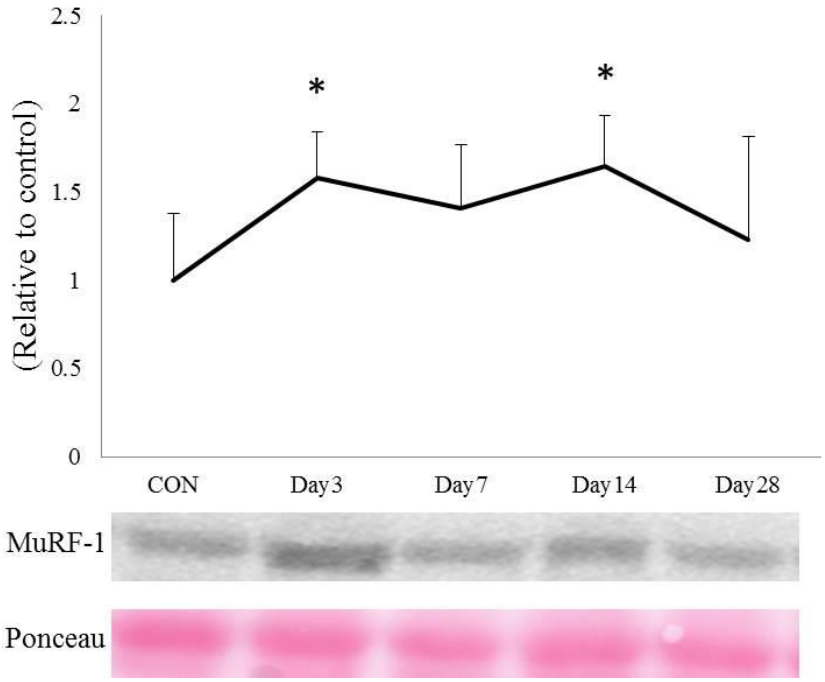

Figure 4-4A. Expression of MuRF-1 until 28 day post-NCI

The values are expressed as mean + SD.

*P < 0.05, vs. CON. Post hoc tests were performed by Fisher exact test

B

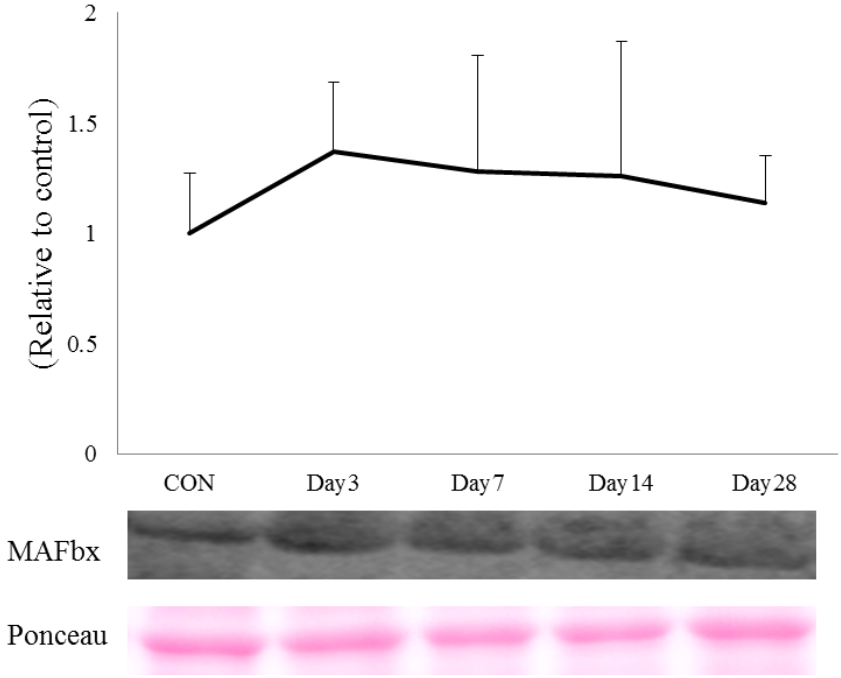

Figure 4-4B. Expression of MAFbx until 28 day post-NCI

The values are expressed as mean + SD.

A

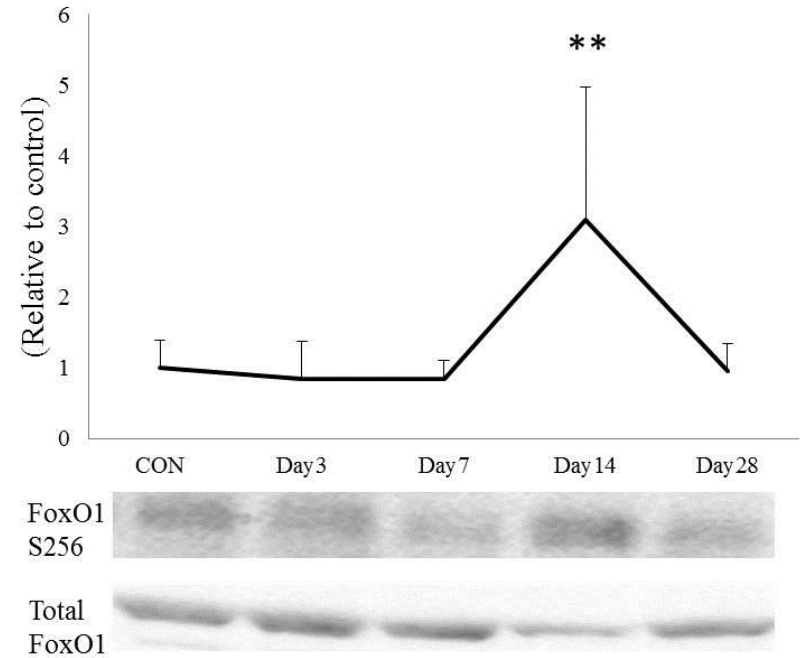

Figure 4-5A. Level of phosphorylated FoxO1 until 28 day post-NCI

The values are expressed as mean + SD.

***P* < 0.01, vs. CON. Post hoc tests were performed by Fisher exact test

B

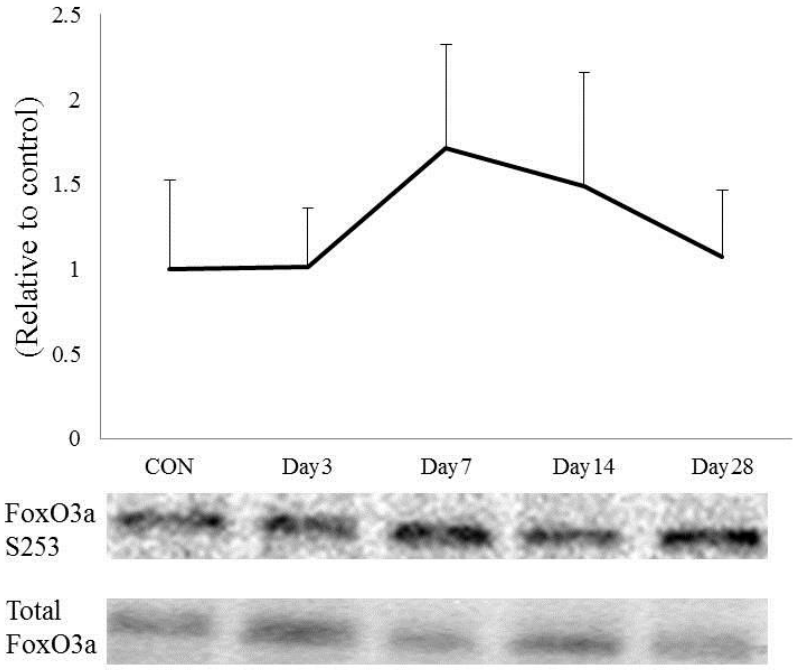

Figure 4-5B. Level of phosphorylated FoxO3a until 28 day post-NCI

The values are expressed as mean + SD.

Chapter 5. Summary and Perspective

5-1 Summary and Perspective

In the chapter 2, I confirmed that 180EC stimulated regulation of FoxO1, FoxO3a, and myostatin activity. Furthermore, I demonstrated that AMPK activation was associated with reduced levels of the phosphorylated forms of FoxO1 and FoxO3a and stimulated myostatin levels. Thus, I conclude that AMPK activation plays an important role in the regulation of FoxO1, FoxO3a, and myostatin activity in case of induced muscle damage by 180EC.

In chapter 3, I observed that 180EC induce nerve damage by confirming a damaged myelin sheath and reduction of NCV as well as muscle damage and protein degradation. Since I can't conclude whether nerve damage by ECs induces AMPK activation and muscle protein degradation, I examined whether nerve damage induces AMPK activation and relate to levels of FoxO1 and FoxO3a and myostatin using a model of NCI in the chapter 4.

As a result, meaning of AMPK activation, phosphorylated ACC was induced and the expression of myostatin was elevated with muscle atrophy. However, AMPK activation did not relate to levels of the phosphorylated forms of FoxO1 and FoxO3a. Thus, I conclude that AMPK is associated with the regulation of myostatin activity, but

phosphorylated states of FoxOs seem to be independent.

In conclusion, 180EC induce not only muscle protein degradation but also nerve damage. Furthermore, AMPK activation and the expression of myostatin have an important role in case of nerve damage induced by 180EC.

In the future, more studies will be necessary to determine whether inhibited AMPK activation and inhibited expression of myostatin support to prevention of muscle protein degradation when nerve is damaged.

Consequently, blocking AMPK activation and the expression of myostatin may be effective for patients with muscle atrophy caused by nerve injury as well as muscle and nerve damage induced by severe ECs.

5-2 Figure

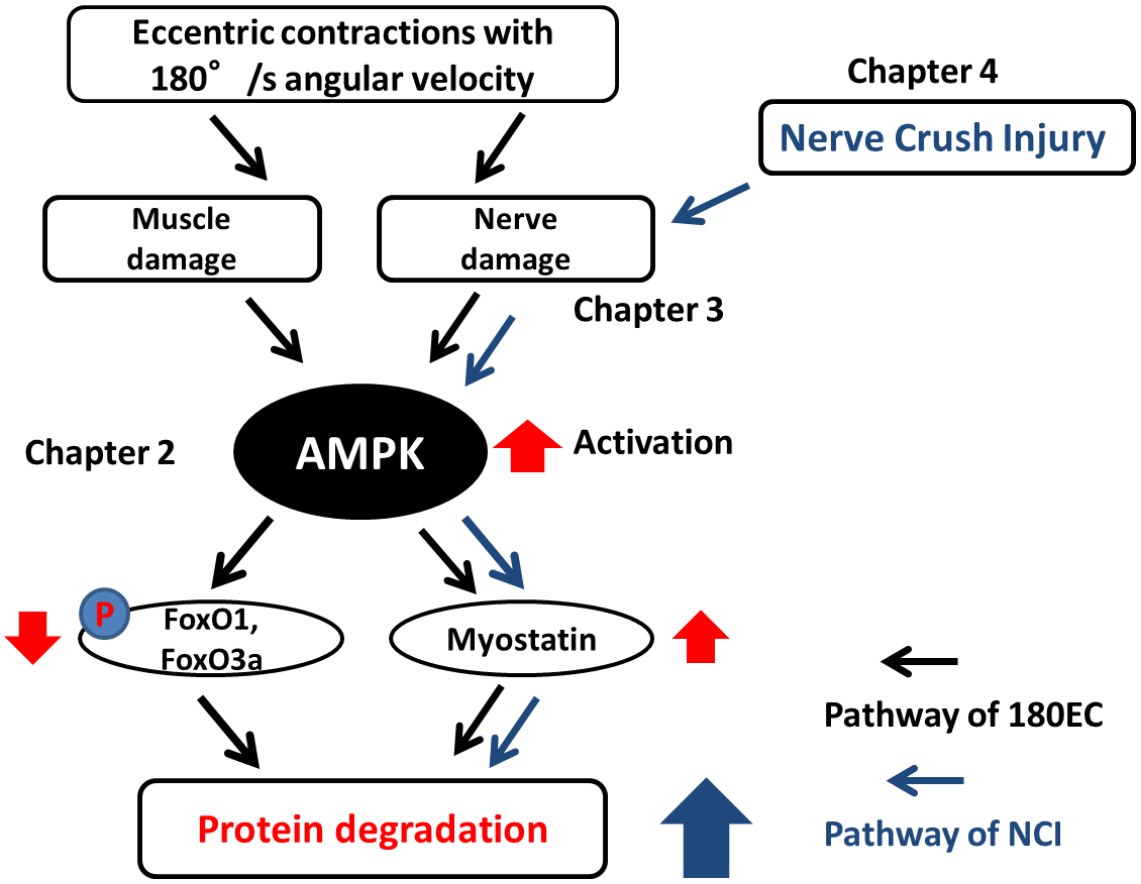

Figure 5-1. Summary diagram

The chapter 2 demonstrated that AMPK activation was associated with regulation of FoxO1, FoxO3a and myostatin activity after 180EC.

In chapter 3, 180EC induced nerve damage as well as muscle damage and protein degradation.

AMPK activation (phosphorylated ACC) and the expression of myostatin by NCI related to muscle atrophy in chapter 4.

In conclusion, 180EC induce not only muscle protein degradation but also nerve damage.

Also, AMPK activation and the expression of myostatin have an important role in case of nerve damage induced by 180EC.

References

1. Sherman DL, Brophy PJ: **Mechanisms of axon ensheathment and myelin growth**. *Nat Rev Neurosci* 2005, **6**(9):683-690.
2. Seddon HJ: **A Classification of Nerve Injuries**. *Br Med J* 1942, **2**(4260):237-239.
3. Bentley CA, Lee KF: **p75 is important for axon growth and schwann cell migration during development**. *J Neurosci* 2000, **20**(20):7706-7715.
4. Corfas G, Velardez MO, Ko CP, Ratner N, Peles E: **Mechanisms and roles of axon-Schwann cell interactions**. *The Journal of neuroscience : the official journal of the Society for Neuroscience* 2004, **24**(42):9250-9260.
5. Martini R, Fischer S, Lopez-Vales R, David S: **Interactions between Schwann cells and macrophages in injury and inherited demyelinating disease**. *Glia* 2008, **56**(14):1566-1577.
6. Proske U, Allen TJ: **Damage to skeletal muscle from eccentric exercise**. *Exercise and sport sciences reviews* 2005, **33**(2):98-104.
7. Paschalis V, Koutedakis Y, Jamurtas AZ, Mougios V, Baltzopoulos V: **Equal volumes of high and low intensity of eccentric exercise in relation to muscle damage and performance**. *Journal of strength and conditioning research / National Strength & Conditioning Association* 2005, **19**(1):184-188.
8. Farthing JP, Chilibeck PD: **The effects of eccentric and concentric training at different velocities on muscle hypertrophy**. *European journal of applied physiology* 2003, **89**(6):578-586.
9. Willems ME, Stauber WT: **Fatigue and recovery at long and short muscle lengths after eccentric training**. *Medicine and science in sports and exercise* 2002, **34**(11):1738-1743.
10. Allen DG: **Eccentric muscle damage: mechanisms of early reduction of force**. *Acta physiologica Scandinavica* 2001, **171**(3):311-319.
11. Proske U, Morgan DL: **Muscle damage from eccentric exercise: mechanism, mechanical signs, adaptation and clinical applications**. *The Journal of physiology* 2001, **537**(Pt 2):333-345.
12. Takekura H, Fujinami N, Nishizawa T, Ogasawara H, Kasuga N: **Eccentric exercise-induced morphological changes in the membrane systems involved in excitation-contraction coupling in rat skeletal muscle**. *The Journal of physiology* 2001, **533**(Pt 2):571-583.
13. Chleboun GS, Howell JN, Conatser RR, Giesey JJ: **Relationship between muscle swelling and stiffness after eccentric exercise**. *Medicine and science in sports and exercise* 1998, **30**(4):529-535.
14. Chen TC, Hsieh SS: **Effects of a 7-day eccentric training period on muscle damage and inflammation**. *Medicine and science in sports and exercise* 2001, **33**(10):1732-1738.

15. Friden J, Lieber RL: **Eccentric exercise-induced injuries to contractile and cytoskeletal muscle fibre components**. *Acta physiologica Scandinavica* 2001, **171**(3):321-326.
16. Warren GL, Hayes DA, Lowe DA, Armstrong RB: **Mechanical factors in the initiation of eccentric contraction-induced injury in rat soleus muscle**. *The Journal of physiology* 1993, **464**:457-475.
17. Garrett WE, Jr.: **Muscle strain injuries**. *Am J Sports Med* 1996, **24**(6 Suppl):S2-8.
18. Chapman D, Newton M, Sacco P, Nosaka K: **Greater muscle damage induced by fast versus slow velocity eccentric exercise**. *International journal of sports medicine* 2006, **27**(8):591-598.
19. Chapman DW, Newton M, McGuigan M, Nosaka K: **Effect of lengthening contraction velocity on muscle damage of the elbow flexors**. *Medicine and science in sports and exercise* 2008, **40**(5):926-933.
20. McCully KK, Faulkner JA: **Injury to skeletal muscle fibers of mice following lengthening contractions**. *J Appl Physiol (1985)* 1985, **59**(1):119-126.
21. Nosaka K, Clarkson PM: **Muscle damage following repeated bouts of high force eccentric exercise**. *Medicine and science in sports and exercise* 1995, **27**(9):1263-1269.
22. Paschalis V, Nikolaidis MG, Giakas G, Jamurtas AZ, Pappas A, Koutedakis Y: **The effect of eccentric exercise on position sense and joint reaction angle of the lower limbs**. *Muscle & nerve* 2007, **35**(4):496-503.
23. Power GA, Dalton BH, Rice CL, Vandervoort AA: **Delayed recovery of velocity-dependent power loss following eccentric actions of the ankle dorsiflexors**. *J Appl Physiol (1985)* 2010, **109**(3):669-676.
24. Song H, Nakazato K, Nakajima H: **Effect of increased excursion of the ankle on the severity of acute eccentric contraction-induced strain injury in the gastrocnemius: an in vivo rat study**. *The American journal of sports medicine* 2004, **32**(5):1263-1269.
25. Ochi E, Hirose T, Hiranuma K, Min SK, Ishii N, Nakazato K: **Elevation of myostatin and FOXOs in prolonged muscular impairment induced by eccentric contractions in rat medial gastrocnemius muscle**. *J Appl Physiol* 2010, **108**(2):306-313.
26. Phillips SM, Glover EI, Rennie MJ: **Alterations of protein turnover underlying disuse atrophy in human skeletal muscle**. *J Appl Physiol (1985)* 2009, **107**(3):645-654.
27. Sorimachi H, Hata S, Ono Y: **Calpain chronicle--an enzyme family under multidisciplinary characterization**. *Proceedings of the Japan Academy Series B, Physical and biological sciences* 2011, **87**(6):287-327.
28. de Palma L, Marinelli M, Pavan M, Orazi A: **Ubiquitin ligases MuRF1 and MAFbx in human skeletal muscle atrophy**. *Joint, bone, spine : revue du rhumatisme* 2008, **75**(1):53-57.
29. Edstrom E, Altun M, Hagglund M, Ulfhake B: **Atrogin-1/MAFbx and MuRF1 are downregulated in aging-related loss of skeletal muscle**. *The journals of gerontology Series A,*

Biological sciences and medical sciences 2006, **61**(7):663-674.

30. Clavel S, Coldefy AS, Kurkdjian E, Salles J, Margaritis I, Derijard B: **Atrophy-related ubiquitin ligases, atrogin-1 and MuRF1 are up-regulated in aged rat Tibialis Anterior muscle**. *Mechanisms of ageing and development* 2006, **127**(10):794-801.
31. Sandri M, Sandri C, Gilbert A, Skurk C, Calabria E, Picard A, Walsh K, Schiaffino S, Lecker SH, Goldberg AL: **Foxo transcription factors induce the atrophy-related ubiquitin ligase atrogin-1 and cause skeletal muscle atrophy**. *Cell* 2004, **117**(3):399-412.
32. Stitt TN, Drujan D, Clarke BA, Panaro F, Timofeyva Y, Kline WO, Gonzalez M, Yancopoulos GD, Glass DJ: **The IGF-1/PI3K/Akt pathway prevents expression of muscle atrophy-induced ubiquitin ligases by inhibiting FOXO transcription factors**. *Molecular cell* 2004, **14**(3):395-403.
33. Tang H, Inoki K, Lee M, Wright E, Khuong A, Khuong A, Sugiarto S, Garner M, Paik J, DePinho RA *et al*: **mTORC1 promotes denervation-induced muscle atrophy through a mechanism involving the activation of FoxO and E3 ubiquitin ligases**. *Science signaling* 2014, **7**(314):ra18.
34. Bodine SC, Stitt TN, Gonzalez M, Kline WO, Stover GL, Bauerlein R, Zlotchenko E, Scrimgeour A, Lawrence JC, Glass DJ *et al*: **Akt/mTOR pathway is a crucial regulator of skeletal muscle hypertrophy and can prevent muscle atrophy in vivo**. *Nature cell biology* 2001, **3**(11):1014-1019.
35. Rommel C, Bodine SC, Clarke BA, Rossman R, Nunez L, Stitt TN, Yancopoulos GD, Glass DJ: **Mediation of IGF-1-induced skeletal myotube hypertrophy by PI(3)K/Akt/mTOR and PI(3)K/Akt/GSK3 pathways**. *Nature cell biology* 2001, **3**(11):1009-1013.
36. McFarlane C, Plummer E, Thomas M, Hennebry A, Ashby M, Ling N, Smith H, Sharma M, Kambadur R: **Myostatin induces cachexia by activating the ubiquitin proteolytic system through an NF-kappaB-independent, FoxO1-dependent mechanism**. *Journal of cellular physiology* 2006, **209**(2):501-514.
37. De Naeyer H, Lamon S, Russell AP, Everaert I, De Spaey A, Vanheel B, Taes Y, Derave W: **Androgenic and estrogenic regulation of Atrogin-1, MuRF1 and myostatin expression in different muscle types of male mice**. *European journal of applied physiology* 2014, **114**(4):751-761.
38. McPherron AC, Lawler AM, Lee SJ: **Regulation of skeletal muscle mass in mice by a new TGF-beta superfamily member**. *Nature* 1997, **387**(6628):83-90.
39. McPherron AC, Lee SJ: **Double muscling in cattle due to mutations in the myostatin gene**. *Proceedings of the National Academy of Sciences of the United States of America* 1997, **94**(23):12457-12461.
40. Kambadur R, Sharma M, Smith TP, Bass JJ: **Mutations in myostatin (GDF8) in**

double-muscled Belgian Blue and Piedmontese cattle. *Genome research* 1997, **7**(9):910-916.

41. Trendelenburg AU, Meyer A, Rohner D, Boyle J, Hatakeyama S, Glass DJ: **Myostatin reduces Akt/TORC1/p70S6K signaling, inhibiting myoblast differentiation and myotube size**. *American journal of physiology Cell physiology* 2009, **296**(6):C1258-1270.
42. Welle SL: **Myostatin and muscle fiber size. Focus on "Smad2 and 3 transcription factors control muscle mass in adulthood" and "Myostatin reduces Akt/TORC1/p70S6K signaling, inhibiting myoblast differentiation and myotube size"**. *American journal of physiology Cell physiology* 2009, **296**(6):C1245-1247.
43. Steinberg GR, Kemp BE: **AMPK in Health and Disease**. *Physiol Rev* 2009, **89**(3):1025-1078.
44. Shaw RJ: **LKB1 and AMP-activated protein kinase control of mTOR signalling and growth**. *Acta Physiol (Oxf)* 2009, **196**(1):65-80.
45. Hardie DG, Sakamoto K: **AMPK: a key sensor of fuel and energy status in skeletal muscle**. *Physiology (Bethesda)* 2006, **21**:48-60.
46. Winder WW, Hardie DG: **Inactivation of acetyl-CoA carboxylase and activation of AMP-activated protein kinase in muscle during exercise**. *Am J Physiol* 1996, **270**(2 Pt 1):E299-304.
47. Hutber CA, Hardie DG, Winder WW: **Electrical stimulation inactivates muscle acetyl-CoA carboxylase and increases AMP-activated protein kinase**. *Am J Physiol* 1997, **272**(2 Pt 1):E262-266.
48. Salt IP, Johnson G, Ashcroft SJ, Hardie DG: **AMP-activated protein kinase is activated by low glucose in cell lines derived from pancreatic beta cells, and may regulate insulin release**. *Biochem J* 1998, **335 (Pt 3)**:533-539.
49. Gordon SE, Lake JA, Westerkamp CM, Thomson DM: **Does AMP-activated protein kinase negatively mediate aged fast-twitch skeletal muscle mass?** *Exerc Sport Sci Rev* 2008, **36**(4):179-186.
50. Williamson DL, Butler DC, Alway SE: **AMPK inhibits myoblast differentiation through a PGC-1alpha-dependent mechanism**. *Am J Physiol Endocrinol Metab* 2009, **297**(2):E304-314.
51. Krawiec BJ, Nystrom GJ, Frost RA, Jefferson LS, Lang CH: **AMP-activated protein kinase agonists increase mRNA content of the muscle-specific ubiquitin ligases MAFbx and MuRF1 in C2C12 cells**. *American journal of physiology Endocrinology and metabolism* 2007, **292**(6):E1555-1567.
52. Thomson DM, Fick CA, Gordon SE: **AMPK activation attenuates S6K1, 4E-BP1, and eEF2 signaling responses to high-frequency electrically stimulated skeletal muscle contractions**. *J Appl Physiol* 2008, **104**(3):625-632.
53. Mounier R, Lantier L, Leclerc J, Sotiropoulos A, Pende M, Daegelen D, Sakamoto K, Foretz M, Viollet B: **Important role for AMPKalpha1 in limiting skeletal muscle cell hypertrophy**.

Faseb J 2009, **23**(7):2264-2273.

54. Nakashima K, Yakabe Y: **AMPK activation stimulates myofibrillar protein degradation and expression of atrophy-related ubiquitin ligases by increasing FOXO transcription factors in C2C12 myotubes**. *Bioscience, biotechnology, and biochemistry* 2007, **71**(7):1650-1656.
55. Allen DL, Unterman TG: **Regulation of myostatin expression and myoblast differentiation by FoxO and SMAD transcription factors**. *Am J Physiol Cell Physiol* 2007, **292**(1):C188-199.
56. Clarkson PM, Nosaka K, Braun B: **Muscle function after exercise-induced muscle damage and rapid adaptation**. *Med Sci Sports Exerc* 1992, **24**(5):512-520.
57. Dartnall TJ, Rogasch NC, Nordstrom MA, Semmler JG: **Eccentric muscle damage has variable effects on motor unit recruitment thresholds and discharge patterns in elbow flexor muscles**. *J Neurophysiol* 2009, **102**(1):413-423.
58. Piitulainen H, Holobar A, Avela J: **Changes in motor unit characteristics after eccentric elbow flexor exercise**. *Scand J Med Sci Sports* 2010.
59. Kami K, Morikawa Y, Kawai Y, Senba E: **Leukemia inhibitory factor, glial cell line-derived neurotrophic factor, and their receptor expressions following muscle crush injury**. *Muscle Nerve* 1999, **22**(11):1576-1586.
60. Stoll G, Griffin JW, Li CY, Trapp BD: **Wallerian degeneration in the peripheral nervous system: participation of both Schwann cells and macrophages in myelin degradation**. *J Neurocytol* 1989, **18**(5):671-683.
61. Yamauchi J, Chan JR, Shooter EM: **Neurotrophin 3 activation of TrkC induces Schwann cell migration through the c-Jun N-terminal kinase pathway**. *Proc Natl Acad Sci U S A* 2003, **100**(24):14421-14426.
62. Bauer J, Ruuls SR, Huitinga I, Dijkstra CD: **The role of macrophage subpopulations in autoimmune disease of the central nervous system**. *Histochem J* 1996, **28**(2):83-97.
63. Bruck W: **The role of macrophages in Wallerian degeneration**. *Brain pathology* 1997, **7**(2):741-752.
64. Venezie RD, Toews AD, Morell P: **Macrophage recruitment in different models of nerve injury: lysozyme as a marker for active phagocytosis**. *J Neurosci Res* 1995, **40**(1):99-107.
65. Stoll G, Jander S: **The role of microglia and macrophages in the pathophysiology of the CNS**. *Prog Neurobiol* 1999, **58**(3):233-247.
66. Baichwal RR, Bigbee JW, DeVries GH: **Macrophage-mediated myelin-related mitogenic factor for cultured Schwann cells**. *Proc Natl Acad Sci U S A* 1988, **85**(5):1701-1705.
67. Chan JR, Cosgaya JM, Wu YJ, Shooter EM: **Neurotrophins are key mediators of the myelination program in the peripheral nervous system**. *Proceedings of the National Academy of Sciences of the United States of America* 2001, **98**(25):14661-14668.
68. Cosgaya JM, Chan JR, Shooter EM: **The neurotrophin receptor p75NTR as a positive**

modulator of myelination. *Science* 2002, **298**(5596):1245-1248.

69. McCall J, Weidner N, Blesch A: **Neurotrophic factors in combinatorial approaches for spinal cord regeneration**. *Cell and tissue research* 2012, **349**(1):27-37.
70. Cui Q: **Actions of neurotrophic factors and their signaling pathways in neuronal survival and axonal regeneration**. *Molecular neurobiology* 2006, **33**(2):155-179.
71. Wilson RS, Ballard LC, Jones ED: **Motor nerve conduction velocity determination in the differential diagnosis of neuromuscular disorders**. *Journal of the National Medical Association* 1962, **54**:174-178.
72. Hudson CH, Dow RS: **Motor Nerve Conduction Velocity Determination**. *Neurology* 1963, **13**:982-988.
73. van Meeteren NL, Brakkee JH, Hamers FP, Helders PJ, Gispen WH: **Exercise training improves functional recovery and motor nerve conduction velocity after sciatic nerve crush lesion in the rat**. *Archives of physical medicine and rehabilitation* 1997, **78**(1):70-77.
74. Ilha J, Araujo RT, Malysz T, Hermel EE, Rigon P, Xavier LL, Achaval M: **Endurance and resistance exercise training programs elicit specific effects on sciatic nerve regeneration after experimental traumatic lesion in rats**. *Neurorehabilitation and neural repair* 2008, **22**(4):355-366.
75. Liu M, Zhang D, Shao C, Liu J, Ding F, Gu X: **Expression pattern of myostatin in gastrocnemius muscle of rats after sciatic nerve crush injury**. *Muscle & nerve* 2007, **35**(5):649-656.
76. Martins RS, Bastos D, Siqueira MG, Heise CO, Teixeira MJ: **Traumatic injuries of peripheral nerves: a review with emphasis on surgical indication**. *Arquivos de neuro-psiquiatria* 2013, **71**(10):811-814.
77. Nakazato K, Song H, Waga T: **Dietary apple polyphenols enhance gastrocnemius function in Wistar rats**. *Med Sci Sports Exerc* 2007, **39**(6):934-940.
78. Nakazato K, Ochi E, Waga T: **Dietary apple polyphenols have preventive effects against lengthening contraction-induced muscle injuries**. *Mol Nutr Food Res* 2010, **54**(3):364-372.
79. Mascher H, Ekblom B, Rooyackers O, Blomstrand E: **Enhanced rates of muscle protein synthesis and elevated mTOR signalling following endurance exercise in human subjects**. *Acta Physiol (Oxf)* 2011, **202**(2):175-184.
80. Fujii N, Hayashi T, Hirshman MF, Smith JT, Habinowski SA, Kaijser L, Mu J, Ljungqvist O, Birnbaum MJ, Witters LA *et al*: **Exercise induces isoform-specific increase in 5'AMP-activated protein kinase activity in human skeletal muscle**. *Biochem Biophys Res Commun* 2000, **273**(3):1150-1155.
81. Chen ZP, Stephens TJ, Murthy S, Canny BJ, Hargreaves M, Witters LA, Kemp BE, McConell GK: **Effect of exercise intensity on skeletal muscle AMPK signaling in humans**. *Diabetes*

2003, **52**(9):2205-2212.

82. Wojtaszewski JF, Nielsen P, Hansen BF, Richter EA, Kiens B: **Isoform-specific and exercise intensity-dependent activation of 5'-AMP-activated protein kinase in human skeletal muscle**. *J Physiol* 2000, **528 Pt 1**:221-226.

83. Stephens TJ, Chen ZP, Canny BJ, Michell BJ, Kemp BE, McConell GK: **Progressive increase in human skeletal muscle AMPKalpha2 activity and ACC phosphorylation during exercise**. *Am J Physiol Endocrinol Metab* 2002, **282**(3):E688-694.

84. Atherton PJ, Babraj J, Smith K, Singh J, Rennie MJ, Wackerhage H: **Selective activation of AMPK-PGC-1alpha or PKB-TSC2-mTOR signaling can explain specific adaptive responses to endurance or resistance training-like electrical muscle stimulation**. *Faseb J* 2005, **19**(7):786-788.

85. Nystrom GJ, Lang CH: **Sepsis and AMPK Activation by AICAR Differentially Regulate FoxO-1, -3 and -4 mRNA in Striated Muscle**. *Int J Clin Exp Med* 2008, **1**(1):50-63.

86. Chen Y, Ye J, Cao L, Zhang Y, Xia W, Zhu D: **Myostatin regulates glucose metabolism via the AMP-activated protein kinase pathway in skeletal muscle cells**. *Int J Biochem Cell Biol* 2010, **42**(12):2072-2081.

87. Zhang C, McFarlane C, Lokireddy S, Bonala S, Ge X, Masuda S, Gluckman PD, Sharma M, Kambadur R: **Myostatin-deficient mice exhibit reduced insulin resistance through activating the AMP-activated protein kinase signalling pathway**. *Diabetologia* 2011, **54**(6):1491-1501.

88. Das AK, Yang QY, Fu X, Liang JF, Duarte MS, Zhu MJ, Trobridge GD, Du M: **AMP-activated protein kinase stimulates myostatin expression in C2C12 cells**. *Biochemical and biophysical research communications* 2012, **427**(1):36-40.

89. Tong JF, Yan X, Zhu MJ, Du M: **AMP-activated protein kinase enhances the expression of muscle-specific ubiquitin ligases despite its activation of IGF-1/Akt signaling in C2C12 myotubes**. *J Cell Biochem* 2009, **108**(2):458-468.

90. Chen BL, Ma YD, Meng RS, Xiong ZJ, Wang HN, Zeng JY, Liu C, Dong YG: **Activation of AMPK inhibits cardiomyocyte hypertrophy by modulating of the FOXO1/MuRF1 signaling pathway in vitro**. *Acta pharmacologica Sinica* 2010, **31**(7):798-804.

91. Greer EL, Oskoui PR, Banko MR, Maniar JM, Gygi MP, Gygi SP, Brunet A: **The energy sensor AMP-activated protein kinase directly regulates the mammalian FOXO3 transcription factor**. *J Biol Chem* 2007, **282**(41):30107-30119.

92. Barthel A, Schmoll D, Kruger KD, Roth RA, Joost HG: **Regulation of the forkhead transcription factor FKHR (FOXO1a) by glucose starvation and AICAR, an activator of AMP-activated protein kinase**. *Endocrinology* 2002, **143**(8):3183-3186.

93. Ochi E, Nakazato K, Ishii N: **Effects of eccentric exercise on joint stiffness and muscle connectin (titin) isoform in the rat hindlimb**. *J Physiol Sci* 2007, **57**(1):1-6.

94. Cameron NE, Cotter MA, Robertson S: **The effect of aldose reductase inhibition on the pattern of nerve conduction deficits in diabetic rats**. *Q J Exp Physiol* 1989, **74**(6):917-926.
95. Hort-Legrand C, Noah L, Meriguet E, Mesangeau D: **Motor and sensory nerve conduction velocities in Yucatan minipigs**. *Laboratory animals* 2006, **40**(1):53-57.
96. Manschot SM, Gispen WH, Kappelle LJ, Biessels GJ: **Nerve conduction velocity and evoked potential latencies in streptozotocin-diabetic rats: effects of treatment with an angiotensin converting enzyme inhibitor**. *Diabetes/metabolism research and reviews* 2003, **19**(6):469-477.
97. Tomita K, Kubo T, Matsuda K, Fujiwara T, Yano K, Winograd JM, Tohyama M, Hosokawa K: **The neurotrophin receptor p75NTR in Schwann cells is implicated in remyelination and motor recovery after peripheral nerve injury**. *Glia* 2007, **55**(11):1199-1208.
98. Al-Bishri A, Forsgren S, Al-Thobaiti Y, Sunzel B, Rosenquist J: **Effect of betamethasone on the degree of macrophage recruitment and nerve growth factor receptor p75 immunoreaction during recovery of the sciatic nerve after injury: an experimental study in rats**. *The British journal of oral & maxillofacial surgery* 2008, **46**(6):455-459.
99. Liao P, Zhou J, Ji LL, Zhang Y: **Eccentric contraction induces inflammatory responses in rat skeletal muscle: role of tumor necrosis factor-alpha**. *Am J Physiol Regul Integr Comp Physiol* 2010, **298**(3):R599-607.
100. Lovering RM, Hakim M, Moorman CT, 3rd, De Deyne PG: **The contribution of contractile pre-activation to loss of function after a single lengthening contraction**. *Journal of biomechanics* 2005, **38**(7):1501-1507.
101. Willems ME, Stauber WT: **Force deficits by stretches of activated muscles with constant or increasing velocity**. *Medicine and science in sports and exercise* 2002, **34**(4):667-672.
102. Tang XF: **[The role of determination of motor and sensory nerve conduction velocity in the diagnosis of diabetic neuropathy]**. *Zhonghua shen jing jing shen ke za zhi = Chinese journal of neurology and psychiatry* 1982, **15**(2):78-81.
103. Ruess JM, Abramson DI, Wasserman RR, Nedvar A: **[Motor nerve conduction velocity in normal and diabetic subjects: effect of repeated periods of ischemia]**. *Archives of physical medicine and rehabilitation* 1973, **54**(5):221-223 passim.
104. Van der Zee CE, Nielander HB, Vos JP, Lopes da Silva S, Verhaagen J, Oestreicher AB, Schrama LH, Schotman P, Gispen WH: **Expression of growth-associated protein B-50 (GAP43) in dorsal root ganglia and sciatic nerve during regenerative sprouting**. *The Journal of neuroscience : the official journal of the Society for Neuroscience* 1989, **9**(10):3505-3512.
105. Belanger E, Henry FP, Vallee R, Randolph MA, Kochevar IE, Winograd JM, Lin CP, Cote D: **In vivo evaluation of demyelination and remyelination in a nerve crush injury model**. *Biomedical optics express* 2011, **2**(9):2698-2708.
106. Gigo-Benato D, Russo TL, Geuna S, Domingues NR, Salvini TF, Parizotto NA: **Electrical**

stimulation impairs early functional recovery and accentuates skeletal muscle atrophy after sciatic nerve crush injury in rats. *Muscle & nerve* 2010, **41**(5):685-693.

107. Jackman RW, Kandarian SC: **The molecular basis of skeletal muscle atrophy**. *Am J Physiol Cell Physiol* 2004, **287**(4):C834-843.

108. Lee K, Kouzaki K, Ochi E, Kobayashi K, Tsutaki A, Hiranuma K, Kami K, Nakazato K: **Eccentric contractions of gastrocnemius muscle-induced nerve damage in rats**. *Muscle & nerve* 2013.

109. Paulsen SR, Rubink DS, Winder WW: **AMP-activated protein kinase activation prevents denervation-induced decline in gastrocnemius GLUT-4**. *Journal of applied physiology* 2001, **91**(5):2102-2108.

110. Gomes AV, Waddell DS, Siu R, Stein M, Dewey S, Furlow JD, Bodine SC: **Upregulation of proteasome activity in muscle RING finger 1-null mice following denervation**. *FASEB journal : official publication of the Federation of American Societies for Experimental Biology* 2012, **26**(7):2986-2999.

111. MacDonald EM, Andres-Mateos E, Mejias R, Simmers JL, Mi R, Park JS, Ying S, Hoke A, Lee SJ, Cohn RD: **Denervation atrophy is independent from Akt and mTOR activation and is not rescued by myostatin inhibition**. *Disease models & mechanisms* 2014, **7**(4):471-481.

References of Table and Figures

Table 1-1. Grades of muscle strain

http://www.radiologyassistant.nl/en/p4a47de30059ba/muscle-mr-traumatic-changes.html

http://www.humankinetics.com/excerpts/excerpts/understanding-muscle-strains

Figure 1-1. The division of tissue layers of skeletal muscle

http://cnx.org/contents/14fb4ad7-39a1-4eee-ab6e-3ef2482e3e22@7.1:65/Anatomy_&_Physiology

Figure 1-2. The components of muscle fiber

http://cnx.org/contents/14fb4ad7-39a1-4eee-ab6e-3ef2482e3e22@7.1:65/Anatomy_&_Physiology

Figure 1-3. The structure of sarcolemma and role of T-tubule and Sarcoplasmic reticulum

http://cnx.org/contents/14fb4ad7-39a1-4eee-ab6e-3ef2482e3e22@7.1:65/Anatomy_&_Physiology

Figure 1-4. The structure of sarcomere and myofibril (thick and thin filament)

http://cnx.org/contents/14fb4ad7-39a1-4eee-ab6e-3ef2482e3e22@7.1:65/Anatomy_&_Physiology

Figure 1-5. The stage of muscle contraction through nerve impulse transmission

https://www.boundless.com/biology/textbooks/boundless-biology-textbook/the-musculoskeletal-system-38/muscle-contraction-and-locomotion-218/excitation-contraction-coupling-828-12071/images/fig-ch38_04_06/

Figure 1-6. The cross section of myelin sheath and axon

http://www.nature.com/nrn/journal/v6/n9/full/nrn1743.html

Figure 1-7. Seddon's classification about nerve injury

http://www.scielo.br/img/revistas/anp/v71n10/0004-282X-anp-71-10-0811-gf01.jpg

Figure 1-8. Major protein degradation systems

http://openi.nlm.nih.gov/detailedresult.php?img=3153876_pjab-87-287-g002&req=4

List of abbreviation

ACC: Acetyl CoA Carboxylase

AICAR: AMPK activator, 5-Aminoimidazole-4-carboxamide ribonucleotide

AMPK: 5′-AMP-Activated Protein Kinase

Akt: Protein kinase B, **PKB**

BDNF: Brain-Derived Neurotrophic Factor

CNS: Central Nervous System

DOMS: Delayed-Onset Muscle Soreness

EC: Eccentric Contraction

ED1: Macrophage related protein

FoxO: Forkhead box O

MAFbx: Muscle-specific ubiquitin ligases muscle atrophy F-box, **Atrogin-1**

mTOR: Mechanistic target of rapamycin

MuRF1: Muscle RING finger 1

NCI: Nerve Crush Injury

NCV: Nerve Conduction Velocity

NGF: Nerve Growth Factor

NT-3: Neurotrophin 3

NT-4/5: Neurotrophin 4/5

PNS: Peripheral Nervous System

p0: Myelin sheath protein zero

TGF: Transforming Growth Factor

Trks: Tropomyosin-Receptor-Kinases

180EC: Eccentric contractions with 180°/s angular velocity

30EC: Eccentric contractions with 30°/s angular velocity

Acknowledgements

This doctoral thesis was carried about in the Graduate School of Health and Sport Science, Nippon Sport Science University (NSSU) for 2010-2015 years.

I would like to thanks to many teachers and coworkers who provide me useful assistance.

Without their assistance, I would not have been able to complete my thesis.

Especially, I am sincerely appreciates professor. Koichi Nakazato. He has provided all the help.

To be specific, he was not only my mentor but also taught me experimental method and expertise.

Also, I gratefully appreciate the financial support the Heiwa Nakazima Foundation (2011-2012) and Sakaguchi International Educating Foundation (2012-2015) that made it possible to complete my thesis.

I am thankful to my senior Hong-sun Song who gives me an opportunity to come to the NSSU.

Finally, I would like to express gratitude to my family that gave me mental support and encouragement.

For five years including a master`s course in Japan, although I had a hard time, it was a valuable experience for me. I would like to remain on my memory past five years for all my life.

List of publication

Lee K, Kouzaki K, Ochi E, Kobayashi K, Tsutaki A, Hiranuma K, Kami K, Nakazato K.

Eccentric contractions of gastrocnemius muscle-induced nerve damage in rats.

Muscle Nerve. 2014 Jul;50 (1):87-94.